



## Original Article

## A novel harbor seal whiskers optimization algorithm



Hegazy Zaher<sup>a</sup>, H. Al-Wahsh<sup>b</sup>, M.H. Eid<sup>b</sup>, Radwa S.A. Gad<sup>b</sup>, Naser Abdel-Rahim<sup>c</sup>, Islam M. Abdelqawee<sup>d</sup>

<sup>a</sup> Faculty of Graduate Studies for Statistical Research, Cairo University, Egypt

<sup>b</sup> Basic Science Dept., Shoubra Faculty of Engineering, Benha University, Egypt

<sup>c</sup> Future University in Egypt, Egypt

<sup>d</sup> Electrical Engineering Dept., Faculty of Engineering at Shoubra, Benha University, Egypt

## ARTICLE INFO

**Keywords:**

Harbor seal whiskers  
Maximum power point  
Optimization  
Photovoltaic  
Partial shading

## ABSTRACT

A novel optimization algorithm, namely Harbor Seal Whiskers Optimization Algorithm (HSWOA) is proposed in this work. Harbor seals use their whiskers to find underwater disturbances which are in the form of oscillating spheres and track prey even though they lack lateral-line systems. HSWOA mimics the high-level sensing that seal whiskers possess. As such, HSWOA has an excellent exploration capability for the search space and a high exploitation capacity for exploiting the all-optimum solutions to reach the most optimum solution. To validate these abilities, the proposed HSWOA utilizes two sets of test functions: 33 benchmark functions and five IEEE Congress on Evolutionary Computation (CEC2019) benchmark functions. The results of HSWOA are compared with ten well-established optimization algorithms. The comparison results show that HSWOA offers superior performance indices to reach an optimum solution while requiring less control variables. The results also show that HSWOA is more efficient regarding computational demand and resolution accuracy. Finally, the HSWOA is employed to track Maximum Power Point (MPP) of Photovoltaic (PV) array with partial shading conditions (PSCs) for two case studies. The results show that HSWOA extracts maximum power in minimum tracking time and high average power capturing capability compared to other optimization techniques.

## 1. Introduction

Numerous optimization strategies have evolved over the past few decades to address a variety of optimization issues. But as human society and contemporary industrial processes have advanced, real-world optimization problems' complexity has grown significantly, posing an even greater difficulty for optimization techniques [1]. The current optimization methods can generally be classified into deterministic and meta-heuristic algorithms. Particular mathematical techniques known as deterministic algorithms operate mechanically and repeatedly without using randomness. A deterministic approach consistently produces the same result for a specific initial input on a given problem. Newton's method and gradient descent algorithm are two well-known deterministic algorithm examples [2]. Although some nonlinear problems can be solved by using such algorithms, they may need derivative information of the problems and have a tendency to get stuck in the local best solutions. As a result, these techniques are useless when tackling complex problems with multiple optimums that are severely constrained [3].

Meta-heuristic methods have developed into the best replacements for deterministic methods. These techniques iteratively explore and utilize the search space using a minimum or maximum function by using various operators [4]. The exploitation and exploration can be balanced using these algorithms [5]. Meta-heuristic methods have been extensively researched over the past 20 years and can be used for many different fields, including engineering design, energy, finance, scheduling, and the economy and trade [6–15]. Owing to their arbitrary nature and black box approach to problems, meta-heuristic methods are particularly popular. Randomness reduces the initial condition sensitivity of meta-heuristics and makes switching between exploration and exploitation easier. Due to the unknowable nature, we can concentrate on the input and output compared to understanding the problems' structural details. Due to these advantages, meta-heuristics can successfully identify globally ideal solutions to issues that Deterministic procedures are unable to address due to a deficiency in derivatives or other relevant information.

The development of bio-inspired algorithms has advanced the most rapidly among meta-heuristic techniques in recent years, and they are increasingly and successfully used to solve various engineering

E-mail address: [radwa.gad@feng.bu.edu.eg](mailto:radwa.gad@feng.bu.edu.eg) (R.S.A. Gad).

| <b>Nomenclature</b>         |   |
|-----------------------------|---|
| <b>Variables</b>            |   |
| $G_{stc}$                   | The irradiance level at STC, 1000 W/m <sup>2</sup>    |
| $I_{D,array}$               | Diode current in single-model of PV array, A          |
| $I_{o,array}$               | Reverse saturation or leakage current of the diode, A |
| $I_{ph,array}$              | PV Photo array current, A                             |
| $I_{PV,array}$              | PV output array current, A                            |
| <b>Abbreviations</b>        |   |
| <b>AHA</b>                  | Artificial Hummingbird Algorithm                      |
| <b>AI</b>                   | Artificial Intelligence                               |
| <b>AM</b>                   | Arithmetic Mean                                       |
| <b>AO</b>                   | Aquila Optimizer                                      |
| <b>APCF</b>                 | Average Power Capturing Factor                        |
| <b>ARO</b>                  | Artificial Rabbits Optimization                       |
| <b>BWO</b>                  | Black Widow Optimization                              |
| <b>CBOA</b>                 | Chef Based Optimization Algorithm                     |
| <b>CEC</b>                  | Congress on Evolutionary Computation                  |
| <b>ChOA</b>                 | Chimp Optimization Algorithm                          |
| <b>CS</b>                   | Cuckoo Search   |
| <b>CSA</b>                  | Crow Search Algorithm                                 |
| <b>DA</b>                   | Dragonfly algorithm                                   |
| <b>DE</b>                   | Differential Evolution                                |
| <b>DLCI</b>                 | leader-Based Collective Intelligence                  |
| <b>EO</b>                   | Equilibrium Optimizer                                 |
| <b>FOA</b>                  | Falcon Optimization Algorithm                         |
| <b>GA</b>                   | Genetic Algorithm                                     |
| <b>GMPP</b>                 | Global Maximum Power Point                            |
| <b>GP</b>                   | Global Peak   |
| <b>GTO</b>                  | Gorilla Troops Optimizer                              |
| <b>GWO</b>                  | Grey Wolf Optimization                                |
| <b>HBA</b>                  | Honey Badger Algorithm                                |
| <b>HAS</b>                  | Harmony Search Algorithm                              |
| <b>HSWOA</b>                | Harbor Seal Whiskers Optimization Algorithm           |
| <b>N<sub>par</sub></b>      | Number of parallel modules in PV array                |
| <b>N<sub>ser</sub></b>      | Number of series modules in PV array                  |
| <b>T<sub>ref</sub></b>      | Cell's Reference temperature, °C                      |
| <b>V<sub>PV,array</sub></b> | The terminal voltage of the PV array, V               |
| <b>IC</b>                   | Incremental Conductance                               |
| <b>JS</b>                   | Jellyfish Search                                      |
| <b>LMPPs</b>                | Local Maximum Power Points                            |
| <b>LPs</b>                  | Local Peaks   |
| <b>MAE</b>                  | Mean Average Error                                    |
| <b>MN</b>                   | Multimodal and Non-Separable                          |
| <b>MPPs</b>                 | Maximum Power Points                                  |
| <b>MPPT</b>                 | Maximum Power Point Tracking                          |
| <b>MS</b>                   | Multimodal and Separable                              |
| <b>MSSA</b>                 | Memetic Salp Swarm Algorithm                          |
| <b>P&amp;O</b>              | Perturb and observe                                   |
| <b>POA</b>                  | Pelican Optimization Algorithm                        |
| <b>PSCs</b>                 | Partial Shading Conditions                            |
| <b>PSO</b>                  | Particle Swarm Optimization                           |
| <b>PV</b>                   | Photovoltaic  |
| <b>RMSE</b>                 | Root Mean Square Error                                |
| <b>RSO</b>                  | Rat Swarm Optimizer                                   |
| <b>SCA</b>                  | Sine Cosine Algorithm                                 |
| <b>SD</b>                   | Standard Deviation                                    |
| <b>SMA</b>                  | Slime Mould Algorithm                                 |
| <b>SOA</b>                  | Seagull Optimization Algorithm                        |
| <b>UN</b>                   | Unimodal and Non-Separable                            |
| <b>US</b>                   | Unimodal and Separable                                |
| <b>WDO</b>                  | Wind Driven Optimization                              |
| <b>WOA</b>                  | Whale Optimization Algorithm                          |

conundrums [16–18]. Bio-inspired algorithms frequently imitate the biological processes of living things and optimally translate them into mathematical models. The following presents a brief description of some of the well-known optimization algorithms. Table 1 highlights the main advantages and disadvantages of many optimization techniques along with some of their applications.

One of the earliest evolutionary algorithms (EAs) is the Genetic Algorithm (GA). The GA was developed by biological systems of natural selection to address challenging optimization issues [19]. Three evolutionary behaviors: selection, crossover, and mutation are imitated in the fundamental form of GA. Each member of the population that makes up the basis of GA represents a potential solution. These three operators change the population over time, and after many iterations, the best individual is used to create a new population. GA converges to the global optimum as a result of the selection of individuals proportional to their fitness values. However, reaching the global optimum depends on the selection of initial conditions [20].

One of the most well-established bio-inspired techniques that emulates the flocking social behaviors of birds is particle swarm optimization (PSO) [21]. The procedure begins with a population of randomly chosen people whose opinions are taken into account to be solutions to a problem. Each individual's position is stochastically updated at each iteration based on the best individual position as well as the best global position for each individual. A person's quality is measured using the function fitness value. Although PSO has a high rate of convergence, it is relatively sensitive to changes in its control parameters and is susceptible to being caught in some high-dimensional problems' local optima [22].

An intriguing bio-inspired algorithm called Cuckoo search (CS) [23] is based on the obligate brood parasitism of some cuckoo species. Two cuckoo behaviors are modelled by CS: breeding and Levy flight. To increase the likelihood that their own eggs will hatch, cuckoos lay their eggs in the nests of host birds and then remove the host birds' eggs. Levy flight offers cuckoos a unique random walk that combines small-scale local search with sporadic long-distance travel and is characterized by the Levy distribution. This approach has been shown to be more effective than PSO and GA at solving some challenging optimization issues [24]. However, CS has some drawbacks, including poor local search performance and low convergence precision [25,26].

The Whale Optimization Algorithm (WOA) is a meta-heuristic algorithm that takes its cues from nature. There are two stages to the search process: exploration and exploitation. The algorithm globally scans the search space in the first stage. The later stage continues the exploration and thoroughly examines the promising area [27].

One of the newest heuristic optimization methods is called Grey Wolf Optimizer (GWO). This method draws its inspiration from the grey wolves' life style, which involves pursuing, attacking, and hunting prey in the wild [28].

An artificial hummingbird algorithm (AHA), a brand-new bio-inspired optimization algorithm, is put forth to address optimization issues. The AHA algorithm mimics the unique flight abilities and cunning foraging techniques of hummingbirds in the wild. Axial, diagonal, and omnidirectional flights are three types of flight abilities used in foraging strategies that are modeled. To model the memory function of hummingbirds for food sources, a visit table is built, along with guided foraging, territorial foraging, and migrating foraging [29].

**Table 1**  
Literature survey for recent metaheuristic techniques.

| Technique                                | Advantages  | Disadvantages   | Application  | Ref. No |
|--|---|---|--|---------|
| Genetic Algorithm (GA)                   | <ul style="list-style-type: none"> <li>The concept is easy to understand.</li> </ul>  | <ul style="list-style-type: none"> <li>Easy to fall into premature convergence, and depends on the initial population.</li> </ul>                                     | Controlling of grid-connected solar farm [19]  | [19,20] |
| Particle Swarm Optimization (PSO)        | <ul style="list-style-type: none"> <li>Fast convergence.</li> <li>High efficiency</li> </ul>  | <ul style="list-style-type: none"> <li>Complex calculation</li> <li>Oscillates during rapidly changing conditions</li> </ul>  | Dynamic global maximum power detection of variant partially shaded PVs [21]                    | [21,22] |
| Cuckoo Search (CS)                       | <ul style="list-style-type: none"> <li>simple for applications</li> <li>Fewer tuning parameters</li> <li>Depend on Levy flights for searching search space</li> </ul>   | <ul style="list-style-type: none"> <li>Fall into local optimal solutions very easily</li> <li>Slow convergence rate</li> </ul>  | MPPT of PVs [23]   | [23–26] |
| Whale Optimization Algorithm (WOA)       | <ul style="list-style-type: none"> <li>Few controls parameters</li> <li>Simple calculation</li> </ul>   | <ul style="list-style-type: none"> <li>Convergence occurs slowly</li> <li>Poor accuracy</li> <li>Simple to slip into a local optimum</li> </ul>                       | MPPT of variable-speed wind generators   | [27]    |
| Grey Wolf Optimizer (GWO)                | <ul style="list-style-type: none"> <li>Fewer variables</li> <li>Simple principles</li> <li>Simple implementation</li> </ul>   | <ul style="list-style-type: none"> <li>Low convergence velocity</li> <li>Poor solution precision</li> <li>Simple to slip into the regional optimum</li> </ul>         | MPPT for photovoltaic system under partial shading conditions                                  | [28]    |
| Artificial Hummingbird Algorithm (AHA)   | <ul style="list-style-type: none"> <li>Excellent handling of single-objective optimization issues</li> </ul>  | <ul style="list-style-type: none"> <li>Slow search speed</li> <li>Low optimization precision</li> <li>Premature convergence</li> </ul>                                | Single-Sensor Global MPPT for Photovoltaic Systems   | [29]    |
| Artificial Rabbits Optimization (ARO)    | <ul style="list-style-type: none"> <li>Simple structure</li> <li>Easy to implement</li> </ul>   | <ul style="list-style-type: none"> <li>Poor accuracy</li> <li>Trapping into local minima</li> </ul>   | Predicting water productivity of different designs of solar stills [30]                        | [30,31] |
| Jellyfish Search (JS) Optimizer          | <ul style="list-style-type: none"> <li>Converges more rapidly</li> <li>Better search performance compared to traditional optimization techniques with fewer algorithmic parameters</li> <li>Keeps exploration and exploitation in better balance</li> </ul> | <ul style="list-style-type: none"> <li>Locked in a local optimum</li> <li>Prematurely converge or take a very long time to converge</li> </ul>                        | Solar energy conversion systems optimization   | [32]    |
| Aquila Optimizer (AO)                    | <ul style="list-style-type: none"> <li>Fast convergence speed</li> <li>High search efficiency</li> <li>Simple structure</li> </ul>  | <ul style="list-style-type: none"> <li>Trapped in local minima</li> </ul>   | monitoring the wind energy conversion system's highest power output                            | [33]    |
| Chef Based Optimization Algorithm (CBOA) | <ul style="list-style-type: none"> <li>Easy to implement</li> </ul>   | <ul style="list-style-type: none"> <li>Easily trapped in local minima</li> </ul>  | Multilevel Thresholding Image Segmentation   | [34]    |
| Coot Optimization Algorithm (COOT)       | <ul style="list-style-type: none"> <li>Simplicity</li> <li>Ease of implementation</li> <li>Few parameters</li> </ul>  | <ul style="list-style-type: none"> <li>Low Convergence</li> </ul>   | Optimal wind energy generation considering climatic variables                                  | [35]    |
| Equilibrium Optimizer (EO)               | <ul style="list-style-type: none"> <li>Simple</li> <li>Robust</li> </ul>  | <ul style="list-style-type: none"> <li>Low convergence velocity</li> <li>A local minimum's convergence</li> </ul>   | Enhancing the performance of fuel cell system  | [36]    |
| Pelican Optimization Algorithm (POA)     | <ul style="list-style-type: none"> <li>Easy to implement</li> </ul>   | <ul style="list-style-type: none"> <li>Trapped into local minima</li> </ul>   | Enhancement of Power Quality in a Renewable Energy System Connected to the Smart Grid          | [37]    |
| Slime Mould Algorithm (SMA)              | <ul style="list-style-type: none"> <li>Increasing the algorithm's speed</li> <li>Reducing the computational memory.</li> </ul>  | <ul style="list-style-type: none"> <li>Unbalanced exploitation and exploration</li> <li>Simple to enter local optimum</li> </ul>                                      | Dynamic structural health monitoring   | [38]    |
| Honey Badger Algorithm (HBA)             | <ul style="list-style-type: none"> <li>High dynamic searchability</li> </ul>  | <ul style="list-style-type: none"> <li>Trapping in local optima due to the population diversity loss</li> </ul>   | Global MPPT for triple-junction solar photovoltaic system under PSCs                           | [39]    |
| Seagull Optimization Algorithm (SOA)     | <ul style="list-style-type: none"> <li>Simple structure</li> <li>Easy implementation</li> </ul>   | <ul style="list-style-type: none"> <li>Easily falling into local optimal</li> <li>Low convergence accuracy for solving complex engineering problems.</li> </ul>       | Parameters estimation of photovoltaic models   | [40]    |
| Chimp Optimization Algorithm (ChOA)      | <ul style="list-style-type: none"> <li>Convergence speed</li> <li>Reduced processing time</li> <li>Reduced complexity</li> </ul>  | <ul style="list-style-type: none"> <li>Difficult because of randomness</li> <li>Greatly influenced by initial solution</li> <li>Unaffordable sampling rate</li> </ul> | Improving the Global Maximum Power Point (GMPP) of PV strings in conditions of partial shading | [41]    |
| Black Widow Optimization Algorithm (BWO) | <ul style="list-style-type: none"> <li>Simple construction</li> <li>Easy to apply</li> </ul>  | <ul style="list-style-type: none"> <li>Stuck in the local minimum</li> <li>Premature convergence in some complicated optimization problems</li> </ul>                 | Getting the most power possible out of solar-PV-powered motors for light electric vehicles     | [42]    |
| Gorilla Troops Optimizer (GTO)           | <ul style="list-style-type: none"> <li>Finding the best solution in a short time</li> </ul>   | <ul style="list-style-type: none"> <li>Does not take into account feature redundancy</li> </ul>   | Hybrid DC–AC Microgrid Energy Management System  | [43]    |
| Crow Search Algorithm (CSA)              | <ul style="list-style-type: none"> <li>Simple structure</li> <li>Few control parameters</li> <li>Easy implementation</li> </ul>   | <ul style="list-style-type: none"> <li>Slow convergence</li> <li>Easy fall into local optimum</li> </ul>  | Control the photovoltaic system's maximum power point in a partially shaded environment.       | [44]    |
| Dragonfly algorithm (DA)                 | <ul style="list-style-type: none"> <li>Very simple</li> <li>Easy to implement</li> <li>Convergence time is reasonable</li> </ul>  | <ul style="list-style-type: none"> <li>Does not take have an internal memory that can cause a local optimum to emerge too soon.</li> </ul>                            | improving the grid-connected wind-solar system's power flow control                            | [45]    |
| Rat Swarm Optimizer (RSO)                | <ul style="list-style-type: none"> <li>Very simple structure</li> <li>Fast convergence rate</li> <li>Easily understood and utilized</li> </ul>  | <ul style="list-style-type: none"> <li>Stuck in local minima when the objective function is complicated and contains a lot of variables</li> </ul>                    | MPPT under partially shaded conditions and load variation for PVs                              | [46]    |

The detour foraging and random hiding tactics used by rabbits in nature served as inspiration for the artificial rabbits optimization (ARO) algorithm. The rabbit is forced to eat the grass next to other rabbits' nests as part of the detour foraging strategy, which can keep predators from finding its nest. A rabbit can use the random hiding strategy to choose at random one of its own burrows to hide in, which can lessen the

likelihood that it will be captured by its enemies. In addition, rabbits' energy will decrease, which will cause them to switch from the detour foraging strategy to the random hiding strategy. In order to create a new optimizer, this study mathematically models such survival techniques [30,31].

A new metaheuristic optimization algorithm is developed that is

motivated by how jellyfish hunt for food in the ocean. This behavior involves initially moving with the current, later moving inside jellyfish swarms, and finally switching between these motions using a time control mechanism. The exploration stage initially starts when jellyfish follow ocean currents to find the best locations. A jellyfish swarm forms over time, and as each jellyfish moves around the swarm to find a better spot using both active and passive motions, the exploitation stage (exploitation stage) is reached. A time control mechanism alternates between these motions in the meantime. The ideal phase, the jellyfish bloom, follows the loop's repetition. The numerical tests have demonstrated that the JS algorithm finds the best value by striking a good balance between exploitation and exploration [32].

Aquila Optimizer (AO), a brand-new alternative meta-heuristic method, has been created. The actions of Aquila in nature are mimicked by this algorithm. The four methods used in the AO to represent optimization procedures are: high soar with vertical stoop to select the search space; contour flight with short glide attack to explore within a diverge search space; low flight with slow descent attack to exploit within a converge search space; and walk and grab prey to swoop [33].

The chef-based optimization algorithm (CBOA), a brand-new meta-heuristic algorithm, is created. Cooking instruction in training programs serves as the primary source of inspiration for CBOA design. To improve the ability of local search in exploitation and global search in exploration, the stages of the cooking training process in various phases are mathematically modeled [34].

It was proposed to use a new swarm-based optimization algorithm that was inspired by the regular and erratic movements of Coot on the water's surface. The primary motivation for developing this optimization algorithm was to take advantage of special characteristics like swarm leadership by a leading group and chain movement at the end of the swarm. [35].

A novel mass balance equation for a control volume served as the basis for the Equilibrium Optimizer (EO), a new physics-based optimization algorithm. High exploratory and exploitative search mechanisms to erratically change solutions are incorporated into the EO algorithm's design [36].

The Pelican Optimization Algorithm (POA), a brand-new swarm-based optimization algorithm, was introduced. The strategy and actions of pelicans during hunting are the primary sources of inspiration for the proposed POA. These actions include diving towards their prey and flapping their wings over the water's surface. After outlining the various POA steps, its mathematical modeling was presented for use in resolving optimization issues [37].

These meta-heuristics are based on complex living things' behaviors things to create various local and global search strategies, giving researchers a wider range of algorithms to address optimization issues in a variety of fields.

This work introduces a new bio-inspired optimizer called Harbor Seal Whiskers Optimization Algorithm (HSWOA). Despite the fact that HSWOA is a type of meta-heuristic, it differs significantly from other algorithms. HSWOA differs significantly from them in that it has a different biological background. HSWOA is inspired by the high sensing ability of seal whiskers in tracking its prey.

With two sets of different numerical test functions, the HSWOA is assessed.; 33 benchmark functions and 5 CEC2019 benchmark functions and its results are contrasted with those of various other meta-heuristic methods. AHA, ARO, PSO, JS, AO, CBOA, COOT, EO, GWO, and POA (see Table 1).

A real case study to validate HSWOA is to apply it for maximum power point tracking (MPPT) of PVs under partial shading conditions (PSCs).

In the case of partially shaded PV panels, on the power-voltage curve of the PV array, there are several maximum power points (MPPs). These points are a single global peak (GP), while the others are local peaks

(LPs). So, the conventional tracking strategy such as perturb and observe (P&O) and incremental conductance (IC) are inefficient in many times [47]. As a large number of research articles on global search algorithms are published each year, there has been a paradigm shift in the field of MPPT algorithms [48]. Numerous studies have been conducted in an effort to create an MPPT algorithm that is reliable and efficient for obtaining the PV panel's maximum operating point [49]. MPPT employs both traditional and artificial intelligence (AI) algorithms [50]. Most conventional algorithms work well when there is constant solar radiation and temperature, but they often lose track of their true maximum operating point when there is fluctuating weather or partial shading [51].

PV systems are not be able to produce the global maximum power especially in PSCs and quickly in changing weather conditions. In order to achieve an effective and efficient MPPT of PV systems under PSCs, the Memetic Salp Swarm Algorithm (MSSA) is used. MSSA has a shorter search time and a more consistent convergence, allowing it to find higher quality optimums. MSSA shows the ability to increase the PV system's ability to generate energy in a variety of weather conditions and during various seasons [52].

Dynamic Leader-Based Collective Intelligence (DLCI) is proposed is proposed for MPPT of PV systems affected by PSCs [53]. In contrast to traditional meta-heuristic algorithms, DLCI is made up of a number of sub-optimizers that work together to fully utilize the optimization capabilities of different searching mechanisms rather than just one. This allows for a much wider exploration phase than is possible with a single searching mechanism. The DLCI sub-optimizer with the current best solution is chosen as the dynamic leader for an effective searching guidance to other sub-optimizers in order to achieve a deeper exploitation. Through the use of DLCI, significant reduction of convergence randomness is achieved. As a result, PV systems operating under PSCs can produce much smaller power fluctuations [53].

A novel method for Global Maximum Power Point (GMPP) tracking based on the falcon optimization algorithm (FOA) is reported [54]. FOA is proposed for reducing steady-state oscillations and increasing convergence speed. FOA has a high-performance measures and can successfully track the GMPP under PSCs. FOA tracks GMPP with a quick tracking speed and a tracking efficiency of over 99% in a variety of environmental conditions [54].

The main contributions of this paper:

- 1) Propose a novel bio-inspired HSWOA.
- 2) The proposed technique is distinguished by its sensing velocity equation which makes it more fast for finding the optimal solution for the problem to be solved. This feature of the proposed technique makes it suitable for applying for applications such that MPPT of PV array under PSCs which needs to take fast action accurately.
- 3) Validation the reliability of HSWOA using two sets of numerical tests.
- 4) Applying HSWOA for MPPT of PVs under PSCs for fast tracking and increasing average power capturing factor.

This paper proposes a novel Harbor Seal Whiskers Optimization Algorithm (HSWOA) applied for maximum power point tracking (MPPT) of photovoltaic (PV) array under partial shading conditions (PSCs). The paper is organized as follows. In Sec. II, we give a description of the inspiration and the basic steps of HSWOA. The effectiveness of HSWOA is demonstrated in Sec. III where its performance is compared with the performance of ten well-established optimization techniques using two types of numerical experiments: 33 benchmark functions and five CEC2019 benchmark functions. The analysis of PV characteristics under both PSCs and conditions of uniform irradiation is presented in Sec. IV. Sec. V discusses the results of HSWOA for MPPT of PVs under PSCs. Conclusions are drawn in Sec. VI.

## 2. The Harbor Seal Whiskers Optimization Algorithm

A bio-inspired optimization algorithm, HSWOA, based on the high sensing ability of seal whiskers in tracking its preys. Most mammals have whiskers, unlike humans. These dense, wiry hairs are extremely sensitive to any movement because the base of each one is densely packed with nerve endings. A marine animal like a seal can feel and examine objects with its whiskers, but it can also sense vibrations in the water. Mammals typically have round, uniformly shaped whiskers. However, almost all seal species have wavy and irregularly shaped whiskers. As the seal swims, the whisker is kept steady by its irregular shape. Only in response to hydrodynamic trails does the whisker vibrate. Harbor seals use their whiskers to find underwater disturbances which are in the form of oscillating spheres and track prey even though they lack lateral-line systems [55]. Fig. 1 shows the prey tracking of Harbor Seal.

A structural diagram of the biologically inspired whisker is shown in Fig. 2. Several whiskers moving together send signals to the nerve in the cheek which are conveyed to the brain of the harbor seal under the stimulation of water flow and allow it to process and interpret complex environments, such as the trails left behind by prey and obstacles [56]. The elliptical cross section of the harbor seal's whisker allows it to distinguish the attack angle from the water flow [57].

The zero angle of attack is the direction where the ellipse's primary axis is parallel to the incoming flow. The whisker will have varied characteristic diameters when the flow of water is coming from several directions, which results in varying drag pressures on the whiskers. Since there are no nerves within whiskers, drag forces will be transferred to cheek tension at the base of whiskers, which will cause sensory signals to be produced for the harbor seal [58–60].

### 2.1. Exploration mode

Harbor seals explore the search space for attacking their preys using their whiskers at a certain sensing velocity. The seal holds its whiskers up and away from its face when tracking underwater vibrations. The movement of a prey stirs up the water. The hydrodynamic trails left by the prey can be picked up by a seal's whiskers, which can also follow the prey's path. This allows the seal to determine the prey's direction, proximity to it, and even its size.

The sensing velocity of the seal whisker is deduced as [61]:

$$v_i = \frac{M}{2\pi} \frac{(2x_i^2 - D^2)}{(x_i^2 + D^2)^{5/2}} \quad (1)$$

and,

$$M = 2\pi\omega sd^3 \sin(\omega t) \quad (2)$$

where  $\omega$ ,  $s$  and  $d$  are the angular frequency, the displacement amplitude, and the oscillating sphere diameter, respectively.  $D$  is the distance between seal and its prey,  $x_i$  is the position of the seal.  $t$  is the time taken by harbor seal to sense the underwater disturbances of prey.

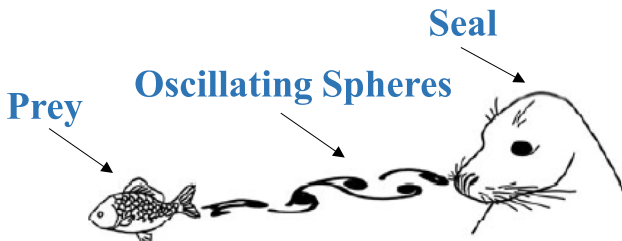


Fig. 1. The prey tracking of Harbor Seal.

### 2.2. Exploitation mode

In this mode, the seals exploit the promising positions of the preys after updating the sensing velocity of whiskers.

The updated sensing velocity is deduced as:

$$v_i^{k+1} = Lr_1 v_i^k + bQr_2(GP_{best} - x_i^k) + aQr_3(LP_{best,i} - x_i^k) \quad (3)$$

$$L = ab^* \frac{1}{\sqrt{b^2 \sin^2 Q + a^2 \cos^2 Q}} \quad (4)$$

$$a = 0.14 \sin(0.92n + 1.5\pi) + 1 \quad (5.a)$$

$$b = 0.067 \sin(0.91n + \pi) - 0.0041n + 0.64 \quad (5.b)$$

where  $L$  is the ellipse diameter,  $r_1$ ,  $r_2$  and  $r_3$  are random numbers,  $a$  is the length of the major axis of the ellipse,  $b$  is the length of the minor axis of the ellipse,  $Q$  is the flowing water attack angle, specifically, the ellipse main axis's angle with the flow velocity direction, and  $n$  is the number of cross sections of one whisker.

The updated position of the seal is

$$x_i^{k+1} = x_i^k + v_i^{k+1} \quad (6)$$

The pseudo code and the flowchart that epitomize the steps of HSWOA are shown in Table 2 and Fig. 3.

## 3. Analysis and results

To successfully verify the HSWOA's performance, two different types of tests are executed, and the optimization results carried out by HSWOA are analyzed and evaluated against those carried out by the other previously mentioned ten algorithms. The first test comprises 33 benchmark functions with a variety of relatively different characteristics inclusive to estimate the performance of comparative optimization algorithms from multiple points of view. The other test is the CEC2019 test that is frequently used to test how well algorithms perform for both exploration and exploitation. These tests are implemented to estimate the effectiveness of the HSWOA. The arithmetic mean of the optimum solution ('AM'), standard deviations ('SD'), root mean square error ('RMSE'), mean average error ('MAE') and average of iteration end over the 50 runs ( $\text{Iter}_{avg}$ ) of the optimum solutions are applied to compare all the comparative techniques, which are formulated as follows:

$$AM = \frac{\sum_{i=1}^{n_r} G_i^*}{n_r} \quad (7)$$

$$SD = \sqrt{\frac{\sum_{i=1}^{n_r} |AM - G_i^*|^2}{n_r}} \quad (8)$$

$$RMSE = \sqrt{\frac{\sum_{i=1}^{n_r} |G_i^* - G_{opt}|^2}{n_r}} \quad (9)$$

$$MAE = \frac{\sum_{i=1}^{n_r} |G_i^* - G_{opt}|}{n_r} \quad (10)$$

where  $G_i^*$  is the best optimum solution obtained in the  $i^{th}$  independent run,  $n_r$  is independent runs number and  $G_{opt}$  is the optimal value of each benchmark function. It is clear that the more reliable and stable outcomes the algorithm can display, lower values of the five evaluation parameters indicate.

The number of population and maximum number of iterations are 50 and 1000 respectively for the proposed technique and all comparative optimizers. The parameter values of each optimizer are described in Table 3. The own parameters of the comparative optimizers are selected

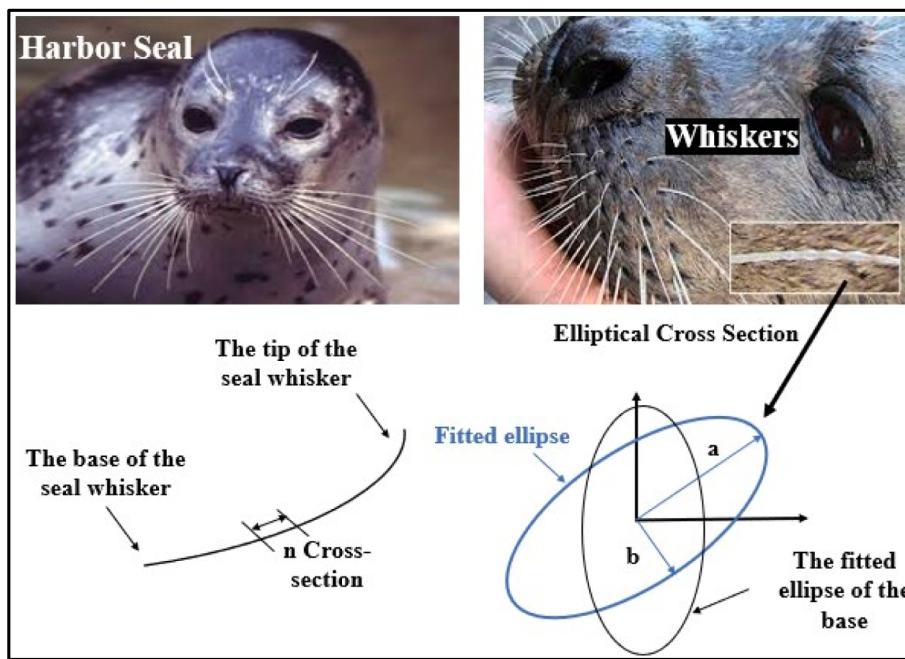


**Fig. 2.** The structural schematic of the bio-inspired whisker.

**Table 2**  
Pseudo code of HSWOA.

- 1- Initialize the parameters such as number of populations  $N_{pop}$ , dimension (dim), and lower boundaries ( $LB$ ) and uppers ( $UB$ ) of the search space, displacement amplitude of the oscillating sphere ( $s$ ), angular frequency of the oscillating sphere ( $w$ ), diameter of the oscillating sphere ( $d$ ), ellipse diameter ( $L$ ), length of the ellipse major axis ( $a$ ), length of the ellipse minor axis ( $b$ ), water flow angle of attack ( $Q$ ).
- 2- Generate random positions ( $x$ ) for whiskers of Harbor Seal.
- 3- Calculate velocity for the whiskers ( $v_t$ ) using Eq. (1).
- 4- While (termination criterion doesn't meet).
- 5- For each whisker in  $x$ .
- 6- Compute the sensing objective function.
- 7- Update the best local whisker position ( $LP_{best,t,i}$ ).
- 8- Update the global best whisker position ( $GP_{best}$ ).
- 9- Update a new Whisker velocity using Eq. (2).
- 10- Update the position of current whisker using Eq. (3).
- 11- End For.
- 12- Return the global best solution ( $G_{best}$ ).

as the optimized values in their main references mentioned in [Table 3](#). The own parameters of HSWOA are selected according to the requirement of high sensing velocity of whiskers to track its prey and based on the position of the seal and its prey. By trial-and-error method, it is obvious the value of  $Q$  is between  $70^\circ$  &  $80^\circ$  to reach to the prey with higher convergence speed. The value of cross sections number of one whisker ( $n$ ) has a big effect on the sensing process of the preys. It is clear that the higher value of  $n$ , the faster the seal reaches to its prey. However, it is noticed by trial-and-error method that the number mustn't be increased than 20 as the sensing velocity will decrease.

All techniques are implemented using MATLAB/Simulink. The capabilities of my computer are Intel(R) Core (TM) i5-5200U CPU @ 2.20 GHz 2.20 GHz with 12.0 GB Ram and 64-bit operating system, x64-based processor using ode23tb solver with 10  $\mu$ s sampling size.

### 3.1. Case study 1: 33 benchmark functions

In this test, 33 benchmark function s represented in [Appendix A](#) are executed and their specifics are available in [\[62\]](#). The four types of functions that are covered by this test are unimodal, multimodal, separable, and non-separable. The multimodal functions have more than

one local extremum in contrast to the unimodal functions' single one, making it simple for algorithms to find the local optimum. The separable property indicates that the function's variables can be divided into a product of every variable of functions, but the non-separable characteristic not enables due to the relationships between their variable which usually makes it difficult to find the global optimum. The functions are 14 unimodal, 19 multimodal, 10 separable, and 23 non-separable. The results of HSWOA are compared with those of ten different swarm-based optimizers, including AHA, ARO, PSO, JS, AO, CBOA, COOT, EO, GWO, and POA. The population size and the number of iterations are set as 50 and 1000 for all considered techniques, which are run 50 times for each function.

The evaluation results of the optimum solutions are presented for each function in [Tables 4–6](#), in which HSWOA offers the best results over on 23 benchmark functions and performs other functions competitively as well. On 13 out of 33 benchmark functions the  $iter_{end}$  of HSWOA is the best over the competitive techniques. HSWOA and AO provide the same  $iter_{end}$  on F1. HSWOA and JS has the best AM, SD, MAE and RMSE on F28 and F32. On 7 out of 33 benchmark functions the  $iter_{end}$  of CBOA is the best over the competitive techniques. ARO provides the best  $iter_{end}$  on F26.

HSWOA has the best AM, SD, MAE and RMSE over all competitive techniques on F4. HSWOA and all competitive techniques provide the same best AM on F15, F20, F22, F25, F26 and F29. HSWOA, AHA, ARO and AO have the same best AM, MAE and RMSE on F31. CBOA has the best AM, MAE and RMSE on F13 and F14. AHA has the best AM, SD, MAE and RMSE on F19 and F27. JS has the best AM, SD, MAE and RMSE on F28.

HSWOA, AHA, PSO and EO have the same best SD on F14. HSWOA, AHA, PSO and EO have the same best SD on F14. HSWOA, AHA, ARO, PSO and JS have the same best SD on F15 and F25. HSWOA, PSO, JS, COOT and EO have the best SD on F26. COOT and AO have the best SD over all competitive techniques on F29 and F31, respectively. EO provides the best SD over all competitive techniques on F14, F20 and F22. CBOA, COOT, EO, GWO and POA provide the best RMSE and MAE on F22.

GWO and COOT provide the best RMSE and MAE on F20 and F26, respectively. AO provides the best RMSE and MAE on F15 and F29. CBOA and EO provide the best RMSE on F25.

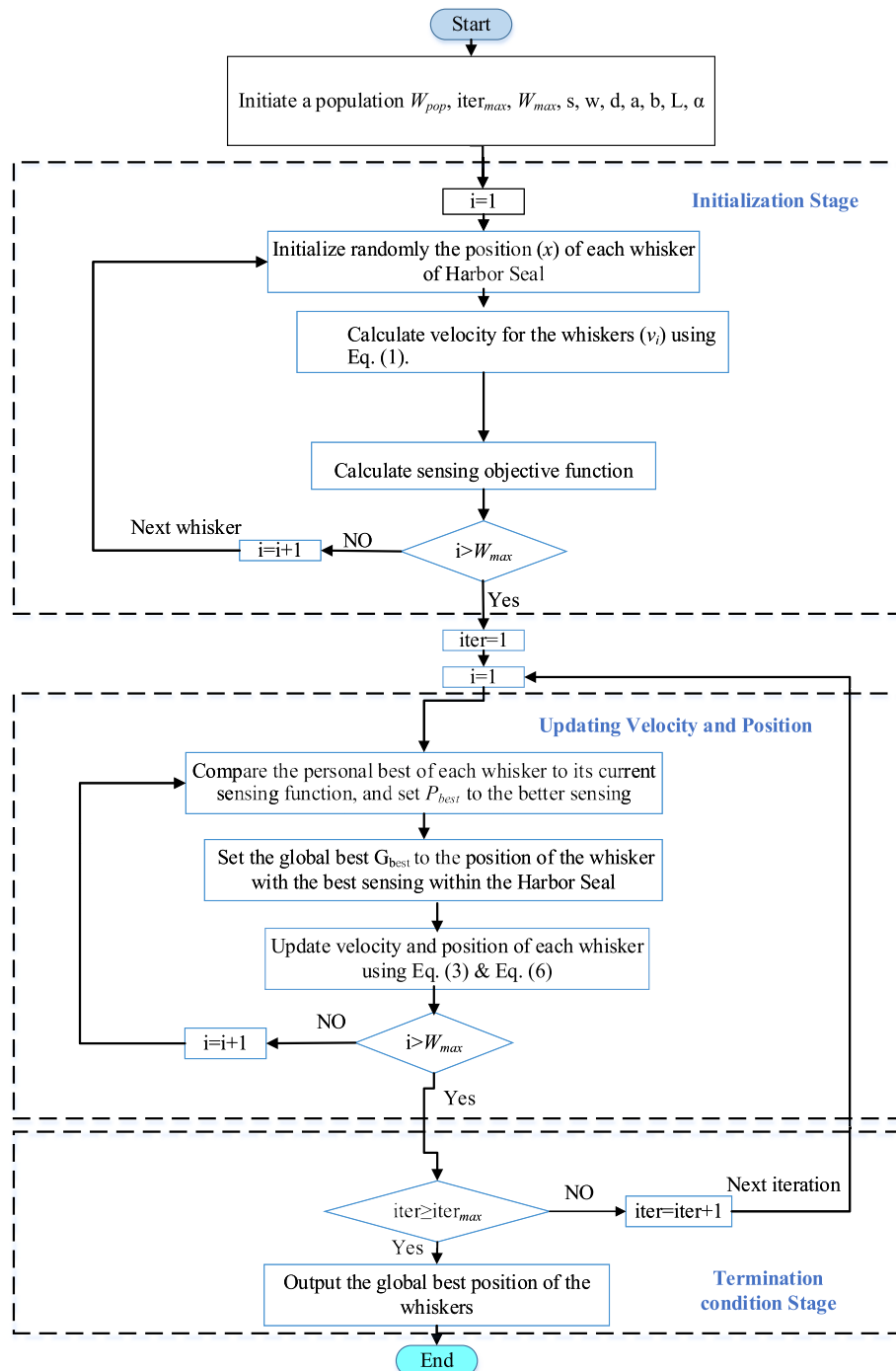


Fig. 3. Flowchart of HSWOA.

The convergence curves of HSWOA versus the other comparative optimizers are provided in Fig. 4. The curves show the best convergence of HSWOA for the most of benchmark functions.

The Count of best hits of HSWOA compared to other techniques is shown in Fig. 5. The figure shows that HSWOA hits the optimal solution of the greatest number of benchmark functions compared to the comparative technique. Comparing to AHA, ARO, PSO, JS, AO, CBOA, COOT, EO, GWO and POA, HSWOA hits 29, 32, 33, 33, 29, 28, 33, 28, 29 and 30 out of 33 functions whereas the comparative optimizers hit 24, 29, 31, 30, 23, 24, 28, 23, 26 and 25 functions, respectively.

### 3.2. Statistical analysis for case study 1

The Wilcoxon signed-rank test [63] is used for better comparison in order to accurately assess the general performance of HSWOA. The Wilcoxon signed-rank test, with a significance level of  $\alpha = 0.05$ , can determine whether HSWOA is superior to the other competitors using the results of 33 functions over 50 runs of each algorithm. Table 7 provides a statistical summary of the Wilcoxon signed-rank test's results for the significance difference. In Table 7, the symbols '=' demonstrates that the HSWOA and the comparative method are not statistically different, '+' means that HSWOA statistically outperforms a different

**Table 3**

Input parameters for each optimization algorithm.

| HWSOA  | AO [33]                              |
|--|--------------------------------------|
| $r_1$ Random value [0,1]                       | $r_1$ Number of search cycles [1:20] |
| $r_2$ Random value [0,1]                       | $D_1$ Random value [1:D]             |
| $r_3$ Random value [0,1]                       | w Constant 0.005                     |
| Q Flowing water attack angle (80/180) × pi     |                                      |
| w angular frequency 2 × pi × 80                |                                      |
| s displacement amplitude 20                    |                                      |
| d oscillating sphere diameter 0.5              |                                      |
| n number of cross sections of one whisker 20   |                                      |
| D Distance between seal and its prey 25        |                                      |
| PSO [22]                                       |                                      |
| W Inertia weight 0.4                           |                                      |
| $r_1$ Random value [0,1]                       |                                      |
| $r_2$ Random value [0,1]                       |                                      |
| $c_1$ Cognitive coefficient 1                  |                                      |
| $c_2$ Social coefficient 1                     |                                      |
| EO [36]  |                                      |
| $a_1$ Constant controls exploration ability 2  |                                      |
| $a_2$ Constant controls exploitation ability 1 |                                      |
| GP Generation probability 0.5                  |                                      |
| GWO [28]                                       |                                      |
| A inherent parameter $2a \times r_1$           |                                      |
| D inherent parameter $2r_2$                    |                                      |
| JS [32]  |                                      |
| $\beta$ Distribution coefficient 3             |                                      |
| $\gamma$ Motion coefficient 0.1                |                                      |
| AHA [29]                                       |                                      |
| $2n$ Migration coefficient                     |                                      |
| COOT [35]                                      |                                      |
| P Constant 0.5                                 |                                      |
| NL Number of leaders 5                         |                                      |
| NCoot Number of Coots 45                       |                                      |
| POA [37]                                       |                                      |
| I Random number 1 or 2                         |                                      |
| R Constant 0.2                                 |                                      |
| CBOA [34]                                      |                                      |
| r Random value [0,1]                           |                                      |

algorithm and the null hypothesis is rejected., and ‘-’ is for the opposite. HWSOA is superior to all other comparative optimizers except AO optimizer for US (unimodal and separable) functions. HWSOA outperforms the competition on the UN (unimodal and non-separable) functions by a wide margin. For MS (multimodal and separable) functions, there is no discernible difference between HWSOA and other optimizers. Despite excellent exploration capability and high exploitation capacity for HWSOA, there is some difficulty for obtaining the optimal solution for the multimodal problems with more than one local optimum. To overcome this limitation, the own parameters of the proposed technique is calculated by trial-and-error method. HWSOA shows significant results for MN (multimodal and non-separable) functions.

The Friedman test [64,65] is used in case study 1 to rank each algorithm’s performance. This test orders each algorithm’s value from lowest to highest in addition to evaluating the significance of the difference between HWSOA and the comparative techniques. The higher the rank of an algorithm, the better it is. The ranks obtained from this test are shown in Table 8 and are based on the average solutions offered by HWSOA and other meta-heuristics. Looking at this table, it is clear that the HWSOA stands out as the top option among the comparisons, with a Friedman test mean rank of 8.61, followed by 8.71 for AHA and the worst value is 15.79 for the COOT optimizer.

Fig. 6 uses a radar chart to show the rankings for each function across all compared algorithm. The ranks are between 1 and 11 for the mentioned 33 benchmark functions. From Fig. 6, it is obvious that HWSOA has the 1st rank for 15 out of 33 functions which is the best number compared to the comparative optimizers.

### 3.3. Statistical Analysis of Case Study 2: CEC2019 benchmark test functions

This recent benchmark suite includes 5 functions that were showed at the CEC conference [66]. These five functions were concocted for an annual optimization competition called “The 100-Digit Challenge”. The dimensionalities of these functions are the same, which is [-100,100]. The CEC2019 functions are represented in Appendix B.

Table 9 shows the Comparison of the HWSOA, AHA, ARO, PSO, JS, AO, CBOA, COOT, EO, GWO, and POA using 5 Functions from the CEC2019 Functions. Results were proceeded using 1000 iterations with 50 runs.

HWSOA, PSO and EO have the best AM over the rest of competitive techniques on CF4. EO and JS have the AM on CF3 and CF5, respectively. EO and JS have the best AM and SD on CF1 and CF2, respectively. CBOA, EO and PSO have the best SD on CF3, CF4 and CF5, respectively. It is obvious that there is a complicity to get the optimal value of some of CEC2019 functions. To overcome this complicity, the own parameters of HWSOA could be optimizely calculated not by trial-and-error method.

## 4. PV modeling and impact of partial shading conditions (PSCs)

A general block diagram of a PVs is shown in Fig. 7. A PV array is shown coupled to a dc-dc boost converter in the circuit diagram, and the MPPT technique regulates the converter duty cycle. The algorithm will track the necessary solar system characteristics, hence adjusting the converter duty cycle as a result. Therefore, the panel always produces its maximum available output power. The output of the converter can then either be delivered to a dc load directly or to an ac load by connecting them via an inverter.

Many solar cells, which are typically formed of silicon material, make up a PV module. When light energy strikes a solar module, the electrons begin to migrate and current begins to flow. Current sources include solar modules. There are many models of solar cells, including the single diode model which has a simple structure and is well-established [67,68]. Fig. 8 shows a single-diode model PV module. The fundamental equations for the PV module are provided below.

$$I_{pv} = N_p * I_{ph} - N_p * I_o * \left[ \exp \left\{ \frac{q^*(V_{pv} + I_{pv} * R_s)}{N_s * A * K * T} \right\} - 1 \right] \quad (11)$$

$$I_{ph} = (I_{sc}(T) + K_i * (T_{ak} - T_{rk})) * \frac{G}{G_{STC}} \quad (12)$$

$$I_o = \left[ I_{sc}(T) - \frac{V_{oc}(T) - I_{sc}(T) * R_s}{R_{sh}} \right] * \exp \left( - \frac{V_{oc}(T)}{A * N_s * V_t} \right) \quad (13)$$

$$V_{oc}(T) = V_{oc} + K_v * (T_{ak} - T_{rk}) \quad (14)$$

$$I_{sc}(T) = I_{sc} + K_i * (T_{ak} - T_{rk}) \quad (15)$$

where  $A$  is the ideality factor of diode,  $K$  is Boltzman’s constant,  $1.3805 * 10^{-23} J/K$ ,  $q$  is electron charge,  $1.6 * 10^{-19} C$ ,  $R_s$  is panel series resistance,  $R_{sh}$  is panel parallel (shunt) resistance,  $V_{oc}$  is open circuit voltage, and  $T_{ak}$  is actual temperature in Kelvin,  $T_{rk}$  The temperature at STC in Kelvin,  $K_v$  is temperature coefficient in of  $V_{oc}$ ,  $K_i$  is temperature coefficient of  $I_{sc}$ ,  $I_{sc}$  is short circuit current, and  $V_t$  is the junction thermal voltage,  $V_t = (K * T_{ak})/q$ .  $G$ ,  $G_{STC}$ : Irradiance levels in both standard test conditions and during normal operation, ( $1000 W/m^2$ ).

The P-V graphs for various temperature and irradiance levels are shown in Fig. 9a, b. The PV operating point therefore fluctuates with the environmental conditions and does not always remain at the maximum operating value, which reduces the power [69]. Therefore, installing more power generators than the necessary demand is preferable, but doing so also raises the cost [70]. As a result, the PVs use a dc-dc converter with an efficient MPPT technique to modify the converter’s duty cycle in accordance with the environmental conditions, tracking the maximum power point throughout all operating conditions. The P-V graph illustrates a single peak power point, which corresponds to the maximum current and voltage, under uniform irradiance. Therefore, the traditional MPPT techniques would be sufficient and reliable for tracking the true MPP.

However, the power output of a shaded panel reduces in comparison to an unshaded panel when some of the PV panels in an array receive non-uniform irradiation and temperature. In order to operate, the shaded panels must absorb a significant portion of the current from the panels that aren’t shaded. The PV panel is harmed by this condition, which is known as hot spot formation [71,72]. Across each panel, a bypass diode is connected in parallel to prevent this situation, as

**Table 4**

Comparisons of optimizers results for 33 benchmark functions (F1–F11).

| Fun. | Index               | HWOA      | AHA       | ARO       | PSO      | JS        | AO        | CBOA     | COOT     | EO         | GWO       | POA        |
|------|---------------------|-----------|-----------|-----------|----------|-----------|-----------|----------|----------|------------|-----------|------------|
| F1   | AM                  | 0         | 0         | 0         | 2.2      | 0         | 0         | 0        | 0        | 0          | 0         | 0          |
|      | SD                  | 0         | 0         | 0         | 2.45     | 0         | 0         | 0        | 0        | 0          | 0         | 0          |
|      | RMSE                | 0         | 0         | 0         | 3.29     | 0         | 0         | 0        | 0        | 0          | 0         | 0          |
|      | MAE                 | 0         | 0         | 0         | 2.2      | 0         | 0         | 0        | 0        | 0          | 0         | 0          |
|      | Iter <sub>avg</sub> | 6         | 9         | 35        | 863      | 68        | 6         | 9        | 55       | 36         | 48        | 23         |
| F2   | AM                  | 0         | 1.64E-289 | 1.09E-124 | 4.20E-39 | 1.89E-40  | 1.16E-257 | 0        | 1.72E-11 | 2.08E-100  | 3.64E-70  | 5.50E-209  |
|      | SD                  | 0         | 0         | 7.46E-124 | 2.20E-38 | 5.57E-40  | 0         | 0        | 1.20E-10 | 1.35E-99   | 7.41E-70  | 0          |
|      | RMSE                | 0         | 0         | 0         | 2.25E-38 | 5.88E-40  | 0         | 0        | 1.22E-10 | 1.36E-99   | 8.26E-70  | 0          |
|      | MAE                 | 0         | 1.64E-289 | 1.09E-124 | 4.20E-39 | 1.89E-40  | 1.16E-257 | 0        | 1.72E-11 | 2.08E-100  | 3.64E-70  | 5.50E-209  |
|      | Iter <sub>avg</sub> | 361       | 1000      | 1000      | 1000     | 1000      | 1000      | 446      | 1000     | 1000       | 1000      | 1000       |
| F3   | AM                  | 0         | 2.95E-294 | 1.15E-127 | 2.54E-02 | 2.54E-41  | 7.61E-233 | 0        | 6.17E-28 | 3.15E-102  | 2.39E-71  | 9.28E-211  |
|      | SD                  | 0         | 0         | 8.85E-127 | 3.48E-02 | 6.98E-41  | 0         | 0        | 4.32E-27 | 1.14E-101  | 5.55E-71  | 1.40E-211  |
|      | RMSE                | 0         | 0         | 8.92E-127 | 4.25E-02 | 7.39E-41  | 0         | 0        | 4.36E-27 | 1.18E-101  | 6.05E-71  | 1.57E-211  |
|      | MAE                 | 0         | 4.91E-294 | 1.91E-127 | 4.23E-02 | 4.23E-41  | 7.61E-233 | 0        | 6.17E-28 | 3.15E-102  | 2.39E-71  | 9.28E-211  |
|      | Iter <sub>avg</sub> | 365       | 999       | 1000      | 1000     | 1000      | 1000      | 444      | 1000     | 1000       | 1000      | 1000       |
| F4   | AM                  | 2.38E-05  | 9.39E-05  | 3.03E-04  | 1.07E-02 | 7.19E-04  | 4.26E-05  | 2.81E-05 | 1.93E-03 | 3.83E-04   | 5.39E-04  | 7.08E-05   |
|      | SD                  | 1.72E-05  | 1.24E-04  | 4.41E-04  | 1.05E-02 | 7.09E-04  | 4.18E-05  | 1.74E-05 | 1.41E-03 | 1.72E-04   | 4.10E-04  | 4.81E-05   |
|      | RMSE                | 2.94E-05  | 1.54E-04  | 5.29E-04  | 1.48E-02 | 9.91E-04  | 5.97E-05  | 3.31E-05 | 2.40E-03 | 4.20E-04   | 6.77E-04  | 8.56E-05   |
|      | MAE                 | 2.38E-05  | 1.57E-04  | 5.06E-04  | 1.79E-02 | 1.20E-03  | 4.26E-05  | 2.81E-05 | 1.93E-03 | 3.83E-04   | 5.39E-04  | 7.08E-05   |
|      | Iter <sub>avg</sub> | 1000      | 1000      | 1000      | 1000     | 1000      | 1000      | 1000     | 1000     | 1000       | 1000      | 1000       |
| F5   | AM                  | 0         | 0         | 0         | 1.52E-02 | 0         | 7.08E-05  | 2.40E-08 | 1.03E-16 | 0          | 2.74E-08  | 0          |
|      | SD                  | 0         | 0         | 0         | 1.07E-01 | 0         | 7.57E-05  | 1.94E-08 | 6.89E-16 | 0          | 2.86E-08  | 0          |
|      | RMSE                | 0         | 0         | 0         | 1.08E-01 | 0         | 1.04E-04  | 3.09E-08 | 6.96E-16 | 0          | 3.96E-08  | 0          |
|      | MAE                 | 0         | 0         | 0         | 1.52E-02 | 0         | 7.08E-05  | 2.40E-08 | 1.03E-16 | 0          | 2.74E-08  | 0          |
|      | Iter <sub>avg</sub> | 115       | 445       | 383       | 192      | 321       | 1000      | 1000     | 980      | 318        | 1000      | 215        |
| F6   | AM                  | -1        | -1        | -1        | -1       | -1        | -1        | -1       | -1       | -1         | -1        | -9.80E-01  |
|      | SD                  | 0         | 0         | 0         | 0        | 0         | 7.59E-06  | 3.27E-10 | 4.59E-16 | 0          | 1.39E-07  | 1.40E-01   |
|      | RMSE                | 0         | 0         | 0         | 0        | 0         | 8.79E-06  | 3.90E-10 | 4.59E-16 | 0          | 2.17E-07  | 1.41E-01   |
|      | MAE                 | 0         | 0         | 0         | 0        | 0         | 4.44E-06  | 2.13E-10 | 1.13E-16 | 0          | 1.67E-07  | 2.00E-02   |
|      | Iter <sub>avg</sub> | 58        | 204       | 155       | 110      | 192       | 1000      | 1000     | 423      | 87         | 1000      | 160        |
| F7   | AM                  | 1.63E-267 | 1.07E-280 | 1.76E-151 | 0        | 2.31E-168 | 4.06E-294 | 0        | 2.87E-29 | 0          | 2.20E-282 | 1.42E-321  |
|      | SD                  | 0         | 0         | 8.34E-151 | 0        | 0         | 0         | 0        | 2.01E-28 | 0          | 0         | 0          |
|      | RMSE                | 0         | 0         | 8.40E-151 | 0        | 0         | 0         | 0        | 2.03E-28 | 0          | 0         | 0          |
|      | MAE                 | 1.63E-267 | 1.07E-280 | 1.76E-151 | 0        | 2.31E-168 | 4.06E-294 | 0        | 2.87E-29 | 0          | 2.20E-282 | 1.42E-321  |
|      | Iter <sub>avg</sub> | 1000      | 1000      | 1000      | 948      | 1000      | 1000      | 356      | 1000     | 788        | 1000      | 971        |
| F8   | AM                  | -50       | -50       | -50       | -50      | -50       | -49.9956  | -49.9999 | -49.9999 | -49.999999 | -49.9999  | -49.999974 |
|      | SD                  | 0         | 0         | 0         | 0        | 0         | 2.83E-03  | 3.14E-08 | 2.13E-07 | 1.07E-13   | 4.34E-05  | 1.64E-05   |
|      | RMSE                | 0         | 0         | 0         | 0        | 0         | 5.25E-03  | 4.59E-08 | 2.37E-07 | 1.43E-13   | 7.92E-05  | 3.05E-05   |
|      | MAE                 | 0         | 0         | 0         | 0        | 0         | 4.42E-03  | 3.36E-08 | 1.04E-07 | 9.55E-14   | 6.63E-05  | 2.58E-05   |
|      | Iter <sub>avg</sub> | 339       | 655       | 701       | 341      | 694       | 1000      | 1000     | 1000     | 794        | 1000      | 1000       |
| F9   | AM                  | 0         | 1.95E-254 | 5.21E-112 | 1.51E-64 | 2.70E-33  | 1.57E-197 | 0        | 5.00E-50 | 5.51E-97   | 2.15E-89  | 4.34E-219  |
|      | SD                  | 0         | 0         | 3.61E-111 | 9.89E-64 | 8.88E-33  | 0         | 0        | 3.50E-49 | 2.58E-96   | 6.22E-89  | 0          |
|      | RMSE                | 0         | 0         | 3.65E-111 | 1.00E-63 | 9.28E-33  | 0         | 0        | 3.53E-49 | 2.64E-96   | 6.58E-89  | 0          |
|      | MAE                 | 0         | 1.95E-254 | 5.21E-112 | 1.51E-64 | 2.70E-33  | 1.57E-197 | 0        | 5.00E-50 | 5.51E-97   | 2.15E-89  | 4.34E-219  |
|      | Iter <sub>avg</sub> | 350       | 1000      | 1000      | 1000     | 1000      | 1000      | 485      | 1000     | 1000       | 1000      | 1000       |
| F10  | AM                  | 0         | 1.13E-288 | 3.96E-121 | 1.60E-04 | 1.02E-05  | 3.48E-202 | 0        | 1.78E-37 | 3.34E-09   | 3.62E-06  | 1.14E-210  |
|      | SD                  | 0         | 0         | 1.93E-120 | 1.60E-04 | 1.88E-05  | 0         | 0        | 1.25E-36 | 1.47E-08   | 4.06E-06  | 0          |
|      | RMSE                | 0         | 0         | 1.94E-120 | 1.85E-04 | 1.97E-05  | 0         | 0        | 1.26E-36 | 1.50E-08   | 5.44E-06  | 0          |
|      | MAE                 | 0         | 1.13E-288 | 3.96E-121 | 1.60E-04 | 1.02E-05  | 3.48E-202 | 0        | 1.78E-37 | 3.34E-09   | 3.62E-06  | 1.14E-210  |
|      | Iter <sub>avg</sub> | 362       | 1000      | 1000      | 1000     | 1000      | 1000      | 581      | 1000     | 1000       | 1000      | 1000       |
| F11  | AM                  | 0         | 1.92E-151 | 2.51E-69  | 1.02E-02 | 2.09E-21  | 6.43E-125 | 0        | 4.34E-18 | 2.19E-57   | 7.56E-41  | 3.18E-105  |
|      | SD                  | 0         | 8.40E-151 | 7.82E-69  | 3.41E-02 | 2.98E-21  | 4.50E-124 | 0        | 3.04E-17 | 3.46E-57   | 1.08E-40  | 1.97E-104  |
|      | RMSE                | 0         | 8.48E-151 | 7.96E-69  | 3.46E-02 | 3.22E-21  | 4.55E-124 | 0        | 3.07E-17 | 4.10E-57   | 1.32E-40  | 2.00E-104  |
|      | MAE                 | 0         | 1.92E-151 | 2.51E-69  | 1.02E-02 | 2.09E-21  | 6.43E-125 | 0        | 4.34E-18 | 2.19E-57   | 7.56E-41  | 3.18E-105  |
|      | Iter <sub>avg</sub> | 706       | 1000      | 1000      | 1000     | 1000      | 1000      | 836      | 1000     | 1000       | 1000      | 1000       |

explained in Fig. 10a, b, which offers an additional method of conduction when partial shading occurs [72]. As illustrated in Fig. 10c, the P-V characteristics graph shows multiple peaks under the partial shading condition, among which only one point is the true maximum power point. These multiple peak points are known as the local maximum power points (LMPPs), and the true MPP is known as the global maximum power point among all of the LMPPs (GMPP). The majority of traditional MPPT techniques are unable to distinguish the GMPP from all of the LMPP. Numerous stochastic, evolutionary, and swarm-based algorithms have been proposed for this purpose, and these algorithms have also been hybridized for more dependable and efficient MPP tracking.

Maximizing the predicted power from the PVs using the following objective function will result in the best value from the PV array under partial shading:

$$P_{pv,array} = I_{pv,array} * V_{pv,array} \quad (16)$$

$$I_{pv,array} = N_p * I_{ph,array} - N_p * I_{o,array} * \left[ \exp \left\{ \frac{q^*(V_{pv} + I_{pv,array} * R_s)}{N_s * A * K * T} \right\} - 1 \right] \quad (17)$$

$$I_{ph,array} = \left( I_{sc}(T)_{array} + K_i * (T_{ak} - T_{rk}) \right) * \frac{G}{G_{STC}} \quad (18)$$

$$I_{o,array} = \left[ I_{sc}(T)_{array} - \frac{V_{oc}(T)_{array} - I_{sc}(T)_{array} * R_s}{R_{sh}} \right] * \exp \left( - \frac{V_{oc}(T)_{array}}{A * N_s * V_t} \right) \quad (19)$$

$$V_{oc}(T, G) = V_{oc} + k_v(T - T_{stc}) + N_s A(T) V_l \ln \left( \frac{G}{G_{stc}} \right) \quad (20)$$

where,

**Table 5**

Comparisons of optimizers results for 33 benchmark functions (F12–F22).

| Fun. | Index               | HWOA             | AHA              | ARO              | PSO              | JS               | AO               | CBOA             | COOT             | EO               | GWO              | POA              |
|------|---------------------|------------------|------------------|------------------|------------------|------------------|------------------|------------------|------------------|------------------|------------------|------------------|
| F12  | AM                  | 0                | 1.51E-270        | 1.45E-94         | 1.53E-01         | 7.27E-39         | 8.98E-219        | 0                | 4.44E-47         | 6.43E-28         | 8.01E-19         | 6.11E-208        |
|      | SD                  | 0                | 0                | 7.90E-94         | 1.57E-01         | 1.88E-38         | 0                | 0                | 3.11E-46         | 2.02E-27         | 3.79E-18         | 0                |
|      | RMSE                | 0                | 0                | 7.94E-94         | 1.80E-01         | 1.93E-38         | 0                | 0                | 3.14E-46         | 2.12E-27         | 3.87E-18         | 0                |
|      | MAE                 | 0                | 1.51E-270        | 1.45E-94         | 1.53E-01         | 7.27E-39         | 8.98E-219        | 0                | 4.44E-47         | 6.43E-28         | 8.01E-19         | 6.11E-208        |
|      | Iter <sub>avg</sub> | 362              | 1000             | 1000             | 1000             | 1000             | 1000             | 540              | 1000             | 1000             | 1000             | 1000             |
| F13  | AM                  | 2.83E+01         | 2.51E+01         | 8.56E-03         | 3.61E+01         | 3.72E+01         | 5.02E-04         | <b>1.30E-04</b>  | 3.16E+01         | 2.39E+01         | 2.66E+01         | 2.76E+01         |
|      | SD                  | 0.281773         | 2.29E-01         | 2.04E-02         | 2.78E+01         | 4.56E+01         | 6.84E-04         | <b>1.13E-04</b>  | 1.38E+01         | 1.91E-01         | 8.02E-01         | 1.02E+00         |
|      | RMSE                | 28.30340         | 2.51E+01         | 2.21E-02         | 4.55E+01         | 4.56E+01         | 8.49E-04         | <b>1.72E-04</b>  | 3.44E+01         | 2.39E+01         | 2.66E+01         | 2.76E+01         |
|      | MAE                 | 2.83E+01         | 2.51E+01         | 8.56E-03         | 3.61E+01         | 3.72E+01         | 5.02E-04         | <b>1.30E-04</b>  | 3.16E+01         | 2.39E+01         | 2.66E+01         | 2.76E+01         |
|      | Iter <sub>avg</sub> | 1000             | 1000             | 1000             | 1000             | 1000             | 1000             | 1000             | 1000             | 1000             | 1000             | 1000             |
| F14  | AM                  | 6.67E-01         | 6.67E-01         | 5.36E-03         | 6.67E-01         | 4.28E-03         | 2.49E-01         | <b>1.56E-04</b>  | 6.76E-01         | 6.67E-01         | 6.67E-01         | 6.67E-01         |
|      | SD                  | <b>6.66E-16</b>  | <b>6.66E-16</b>  | 3.25E-03         | <b>6.66E-16</b>  | 1.24E-02         | 1.65E-04         | 4.59E-05         | 4.04E-02         | <b>6.05E-16</b>  | 1.07E-05         | 3.03E-06         |
|      | RMSE                | 0.667            | 6.67E-01         | 6.27E-03         | 6.67E-01         | 1.31E-02         | 2.49E-01         | <b>1.63E-04</b>  | 6.77E-01         | 6.67E-01         | 6.67E-01         | 6.67E-01         |
|      | MAE                 | 6.67E-01         | 6.67E-01         | 5.36E-03         | 6.67E-01         | 4.28E-03         | 2.49E-01         | <b>1.56E-04</b>  | 6.76E-01         | 6.67E-01         | 6.67E-01         | 6.67E-01         |
|      | Iter <sub>avg</sub> | 1000             | 1000             | 1000             | 1000             | 1000             | 1000             | 1000             | 1000             | 1000             | 1000             | 1000             |
| F15  | AM                  | <b>3.98E-01</b>  |
|      | SD                  | <b>1.67E-16</b>  |
|      | RMSE                | 1.13E-04         | 1.13E-04         | 1.13E-04         | 1.13E-04         | 1.13E-04         | 1.13E-04         | <b>8.53E-05</b>  | 1.13E-04         | 1.13E-04         | 1.13E-04         | 1.13E-04         |
|      | MAE                 | 1.13E-04         | 1.13E-04         | 1.13E-04         | 1.13E-04         | 1.13E-04         | 1.13E-04         | <b>3.62E-05</b>  | 1.13E-04         | 1.13E-04         | 1.13E-04         | 1.13E-04         |
|      | Iter <sub>avg</sub> | 1000             | 1000             | 1000             | 1000             | 1000             | 1000             | 1000             | 1000             | 1000             | 1000             | 1000             |
| F16  | AM                  | 0                | 0                | 0                | 0                | 0                | 0                | 0                | 1.78E-17         | 0                | 0                | 0                |
|      | SD                  | 0                | 0                | 0                | 0                | 0                | 0                | 0                | 9.77E-17         | 0                | 0                | 0                |
|      | RMSE                | 0                | 0                | 0                | 0                | 0                | 0                | 0                | 9.93E-17         | 0                | 0                | 0                |
|      | MAE                 | 0                | 0                | 0                | 0                | 0                | 0                | 0                | 1.78E-17         | 0                | 0                | 0                |
|      | Iter <sub>avg</sub> | 52               | 48               | 87               | 112              | 118              | 48               | <b>16</b>        | 182              | 40               | 32               | 62               |
| F17  | AM                  | 0                | 0                | 0                | 0                | 0                | 7.39E-05         | 2.68E-10         | 3.36E-16         | 0                | 8.82E-08         | 0                |
|      | SD                  | 0                | 0                | 0                | 0                | 0                | 7.51E-05         | 2.80E-10         | 1.43E-15         | 0                | 7.73E-08         | 0                |
|      | RMSE                | 0                | 0                | 0                | 0                | 0                | 1.05E-04         | 3.88E-10         | 1.47E-15         | 0                | 1.17E-07         | 0                |
|      | MAE                 | 0                | 0                | 0                | 0                | 0                | 7.39E-05         | 2.68E-10         | 3.36E-16         | 0                | 8.82E-08         | 0                |
|      | Iter <sub>avg</sub> | 93               | 392              | 295              | 154              | 340              | 1000             | 1000             | 964              | 204              | 1000             | 200              |
| F18  | AM                  | 0                | 0                | 0                | 5.12E+01         | 9.30E+00         | 6.18E-06         | 0                | 2.61E-14         | 0                | 1.18E-01         | 0                |
|      | SD                  | 0                | 0                | 0                | 1.77E+01         | 5.06E+00         | 4.33E-05         | 0                | 6.75E-14         | 0                | 8.23E-01         | 0                |
|      | RMSE                | 0                | 0                | 0                | 5.42E+01         | 1.06E+01         | 4.37E-05         | 0                | 7.23E-14         | 0                | 8.32E-01         | 0                |
|      | MAE                 | 0                | 0                | 0                | 5.12E+01         | 9.30E+00         | 6.18E-06         | 0                | 2.61E-14         | 0                | 1.18E-01         | 0                |
|      | Iter <sub>avg</sub> | 20               | 55               | 132              | 1000             | 975              | 50               | 29               | 400              | 140              | 285              | 91               |
| F19  | AM                  | -2.77E+03        | <b>-1.24E+04</b> | -1.10E+04        | -6.65E+03        | -7.12E+03        | -8.89E+03        | -1.21E+04        | -7.91E+03        | -9.08E+03        | -6.21E+03        | -7.68E+03        |
|      | SD                  | 3.74E+02         | <b>2.40E+02</b>  | 4.33E+02         | 8.66E+02         | 1.01E+03         | 3.57E+03         | 4.45E+02         | 6.32E+02         | 7.88E+02         | 8.42E+02         | 6.24E+02         |
|      | RMSE                | 9.80E+03         | <b>2.70E+02</b>  | 1.58E+03         | 5.99E+03         | 5.54E+03         | 5.13E+03         | 6.74E+02         | 4.70E+03         | 3.58E+03         | 6.42E+03         | 4.93E+03         |
|      | MAE                 | 9.80E+03         | <b>1.24E+02</b>  | 1.52E+03         | 5.92E+03         | 5.45E+03         | 3.68E+03         | 5.07E+02         | 4.66E+03         | 3.49E+03         | 6.36E+03         | 4.89E+03         |
|      | Iter <sub>avg</sub> | 1000             | 1000             | 1000             | 1000             | 1000             | 1000             | 1000             | 1000             | 1000             | 1000             | 1000             |
| F20  | AM                  | <b>-1.80E+00</b> |
|      | SD                  | 1.78E-15         | 1.78E-15         | 1.78E-15         | 1.78E-15         | 1.78E-15         | 3.00E-04         | 1.78E-09         | 1.24E-15         | <b>1.11E-15</b>  | 5.69E-07         | <b>1.11E-15</b>  |
|      | RMSE                | 1.30E-03         | 1.30E-03         | 1.30E-03         | 1.30E-03         | 1.30E-03         | 4.82E-04         | 3.41E-06         | 3.41E-06         | <b>2.88E-06</b>  | 3.41E-06         |                  |
|      | MAE                 | 1.30E-03         | 1.30E-03         | 1.30E-03         | 1.30E-03         | 1.30E-03         | 3.77E-04         | 3.41E-06         | 3.41E-06         | <b>2.82E-06</b>  | 3.41E-06         |                  |
|      | Iter <sub>avg</sub> | 1000             | 1000             | 1000             | 1000             | 1000             | 1000             | 1000             | 1000             | 1000             | 1000             | 1000             |
| F21  | AM                  | 0                | 0                | 0                | 0                | 0                | 0                | 0                | 0                | 0                | 0                | 0                |
|      | SD                  | 0                | 0                | 0                | 0                | 0                | 0                | 0                | 0                | 0                | 0                | 0                |
|      | RMSE                | 0                | 0                | 0                | 0                | 0                | 0                | 0                | 0                | 0                | 0                | 0                |
|      | MAE                 | 0                | 0                | 0                | 0                | 0                | 0                | 0                | 0                | 0                | 0                | 0                |
|      | Iter <sub>avg</sub> | 54               | 44               | 101              | 100              | 378              | 30               | 19               | 155              | 45               | 29               | 73               |
| F22  | AM                  | <b>-1.03E+00</b> |
|      | SD                  | 6.66E-16         | 6.66E-16         | 6.66E-16         | 6.66E-16         | 6.66E-16         | 1.30E-04         | 9.25E-12         | 7.31E-16         | <b>2.35E-16</b>  | 2.89E-09         | 3.20E-16         |
|      | RMSE                | 1.63E-03         | 1.63E-03         | 1.63E-03         | 1.63E-03         | 1.63E-03         | 1.76E-04         | <b>1.55E-06</b>  | <b>1.55E-06</b>  | <b>1.55E-06</b>  | <b>1.55E-06</b>  | <b>1.55E-06</b>  |
|      | MAE                 | 1.63E-03         | 1.63E-03         | 1.63E-03         | 1.63E-03         | 1.63E-03         | 1.18E-04         | <b>1.55E-06</b>  | <b>1.55E-06</b>  | <b>1.55E-06</b>  | <b>1.55E-06</b>  | <b>1.55E-06</b>  |
|      | Iter <sub>avg</sub> | 1000             | 1000             | 1000             | 1000             | 1000             | 1000             | 1000             | 1000             | 1000             | 1000             | 1000             |

**Table 6**

Comparisons of optimizers results for 33 benchmark functions (F23–F33).

| Fun. | Index               | HWOA      | AHA       | ARO       | PSO       | JS        | AO        | CBOA      | COOT      | EO        | GWO       | POA       |
|------|---------------------|-----------|-----------|-----------|-----------|-----------|-----------|-----------|-----------|-----------|-----------|-----------|
| F23  | AM                  | 0         | 0         | 0         | 0         | 0         | 0         | 0         | 3.89E-17  | 0         | 0         | 0         |
|      | SD                  | 0         | 0         | 0         | 0         | 0         | 0         | 0         | 1.90E-16  | 0         | 0         | 0         |
|      | RMSE                | 0         | 0         | 0         | 0         | 0         | 0         | 0         | 1.94E-16  | 0         | 0         | 0         |
|      | MAE                 | 0         | 0         | 0         | 0         | 0         | 0         | 0         | 3.89E-17  | 0         | 0         | 0         |
|      | Iter <sub>avg</sub> | 54        | 51        | 91        | 114       | 112       | 38        | 17        | 282       | 41        | 34        | 64        |
| F24  | AM                  | 0         | 0         | 0         | 0         | 0         | 0         | 0         | 2.33E-17  | 0         | 0         | 0         |
|      | SD                  | 0         | 0         | 0         | 0         | 0         | 0         | 0         | 1.12E-16  | 0         | 0         | 0         |
|      | RMSE                | 0         | 0         | 0         | 0         | 0         | 0         | 0         | 1.14E-16  | 0         | 0         | 0         |
|      | MAE                 | 0         | 0         | 0         | 0         | 0         | 0         | 0         | 2.33E-17  | 0         | 0         | 0         |
|      | Iter <sub>avg</sub> | 62        | 53        | 111       | 123       | 158       | 71        | 21        | 281       | 51        | 38        | 60        |
| F25  | AM                  | -1.87E+02 |
|      | SD                  | 8.53E-14  | 8.53E-14  | 8.53E-14  | 8.53E-14  | 8.53E-14  | 9.07E-02  | 1.64E-08  | 2.79E-04  | 1.04E-13  | 8.83E-02  | 1.03E-13  |
|      | RMSE                | 2.70E-01  | 2.70E-01  | 2.70E-01  | 2.70E-01  | 2.70E-01  | 1.15E-01  | 9.09E-04  | 9.11E-04  | 9.09E-04  | 9.06E-02  | 9.09E-04  |
|      | MAE                 | 9.09E-04  | 9.09E-04  | 9.09E-04  | 9.09E-04  | 9.09E-04  | 7.01E-02  | 9.09E-04  | 8.67E-04  | 9.09E-04  | 2.03E-02  | 9.09E-04  |
|      | Iter <sub>avg</sub> | 1000      | 1000      | 1000      | 1000      | 1000      | 1000      | 1000      | 1000      | 1000      | 1000      | 1000      |
| F26  | AM                  | 3.00E+00  | 3.00E+00  | 3.00E+00  | 3.00E+00  | 3.00E+00  | 3.01E+00  | 3.00E+00  | 3.00E+00  | 3.00E+00  | 3.00E+00  | 3.00E+00  |
|      | SD                  | 1.13E-14  | 1.14E-14  | 2.38E-14  | 1.13E-14  | 1.13E-14  | 9.93E-03  | 6.40E-11  | 1.13E-14  | 1.13E-14  | 4.07E-06  | 1.58E-14  |
|      | RMSE                | 7.74E-14  | 7.74E-14  | 7.46E-14  | 7.74E-14  | 7.74E-14  | 1.39E-02  | 7.97E-11  | 6.97E-14  | 7.74E-14  | 5.31E-06  | 7.68E-14  |
|      | MAE                 | 7.66E-14  | 7.66E-14  | 7.08E-14  | 7.66E-14  | 7.66E-14  | 9.76E-03  | 4.75E-11  | 6.87E-14  | 7.66E-14  | 3.41E-06  | 7.53E-14  |
|      | Iter <sub>avg</sub> | 981       | 983       | 911       | 982       | 982       | 1000      | 1000      | 982       | 982       | 1000      | 964       |
| F27  | AM                  | 3.16E-04  | 3.07E-04  | 5.12E-04  | 2.12E-03  | 5.12E-04  | 4.15E-04  | 3.58E-04  | 3.28E-04  | 1.63E-03  | 2.80E-03  | 3.33E-04  |
|      | SD                  | 2.62E-05  | 2.24E-19  | 2.65E-04  | 5.17E-03  | 2.65E-04  | 7.31E-05  | 1.73E-04  | 1.28E-04  | 4.74E-03  | 6.49E-03  | 1.80E-04  |
|      | RMSE                | 2.69E-05  | 2.51E-06  | 3.25E-06  | 5.21E-03  | 3.25E-06  | 1.28E-04  | 1.80E-04  | 1.30E-04  | 4.92E-03  | 6.95E-03  | 1.82E-04  |
|      | MAE                 | 6.10E-06  | 2.51E-06  | 4.19E-06  | 1.61E-03  | 4.19E-06  | 1.05E-04  | 4.81E-05  | 1.82E-05  | 1.32E-03  | 2.49E-03  | 2.32E-05  |
|      | Iter <sub>avg</sub> | 1000      | 1000      | 1000      | 1000      | 1000      | 1000      | 1000      | 1000      | 1000      | 1000      | 1000      |
| F28  | AM                  | 4.18E-02  | 3.39E-02  | 2.10E-02  | 5.88E-02  | 1.39E-02  | 1.05E+00  | 5.51E-02  | 1.09E-01  | 9.32E-02  | 7.66E-01  | 2.06E-02  |
|      | SD                  | 7.82E-02  | 9.60E-02  | 7.02E-02  | 1.15E-01  | 2.28E-02  | 1.32E+00  | 1.14E-01  | 1.58E-01  | 1.37E-01  | 7.48E-01  | 6.84E-02  |
|      | RMSE                | 8.86E-02  | 1.02E-01  | 7.33E-02  | 1.29E-01  | 2.67E-02  | 1.68E+00  | 1.27E-01  | 1.92E-01  | 1.66E-01  | 1.07E+00  | 7.14E-02  |
|      | MAE                 | 4.18E-02  | 3.39E-02  | 2.10E-02  | 5.88E-02  | 1.39E-02  | 1.05E+00  | 5.51E-02  | 1.09E-01  | 9.32E-02  | 7.66E-01  | 2.06E-02  |
|      | Iter <sub>avg</sub> | 1000      | 1000      | 1000      | 1000      | 1000      | 1000      | 1000      | 1000      | 1000      | 1000      | 1000      |
| F29  | AM                  | -3.86E+00 |
|      | SD                  | 3.11E-15  | 3.11E-15  | 3.11E-15  | 3.11E-15  | 3.11E-15  | 1.88E-03  | 4.55E-05  | 2.50E-15  | 3.04E-15  | 3.03E-03  | 2.93E-15  |
|      | RMSE                | 2.78E-03  | 2.78E-03  | 2.78E-03  | 2.78E-03  | 2.78E-03  | 1.97E-03  | 2.77E-03  | 2.78E-03  | 2.78E-03  | 3.24E-03  | 2.78E-03  |
|      | MAE                 | 2.78E-03  | 2.78E-03  | 2.78E-03  | 2.78E-03  | 2.78E-03  | 6.08E-04  | 2.77E-03  | 2.78E-03  | 2.78E-03  | 1.13E-03  | 2.78E-03  |
|      | Iter <sub>avg</sub> | 1000      | 1000      | 1000      | 1000      | 1000      | 1000      | 1000      | 1000      | 1000      | 1000      | 1000      |
| F30  | AM                  | 0         | 0         | 0         | 2.94E-02  | 0         | 0         | 0         | 2.40E-16  | 0         | 1.18E-03  | 0         |
|      | SD                  | 0         | 0         | 0         | 3.16E-02  | 0         | 0         | 0         | 1.08E-15  | 0         | 3.68E-03  | 0         |
|      | RMSE                | 0         | 0         | 0         | 3.59E-02  | 0         | 0         | 0         | 1.11E-15  | 0         | 3.87E-03  | 0         |
|      | MAE                 | 0         | 0         | 0         | 2.94E-02  | 0         | 0         | 0         | 2.40E-16  | 0         | 1.18E-03  | 0         |
|      | Iter <sub>avg</sub> | 20        | 66        | 153       | 984       | 264       | 36        | 31        | 407       | 146       | 253       | 94        |
| F31  | AM                  | 8.88E-16  | 8.88E-16  | 8.88E-16  | 8.53E-01  | 6.00E-15  | 8.88E-16  | 9.59E-16  | 5.66E-09  | 4.58E-15  | 1.28E-14  | 3.66E-15  |
|      | SD                  | 8.87E-31  | 8.87E-31  | 8.87E-31  | 7.81E-01  | 1.76E-15  | 0.00E+00  | 4.97E-16  | 3.96E-08  | 6.96E-16  | 2.73E-15  | 1.47E-15  |
|      | RMSE                | 8.88E-16  | 8.88E-16  | 8.88E-16  | 1.16E+00  | 6.26E-15  | 8.88E-16  | 1.08E-15  | 4.00E-08  | 4.64E-15  | 1.31E-14  | 3.94E-15  |
|      | MAE                 | 8.88E-16  | 8.88E-16  | 8.88E-16  | 8.53E-01  | 6.00E-15  | 8.88E-16  | 9.59E-16  | 5.66E-09  | 4.58E-15  | 1.28E-14  | 3.66E-15  |
|      | Iter <sub>avg</sub> | 1000      | 1000      | 1000      | 1000      | 1000      | 1000      | 1000      | 1000      | 1000      | 1000      | 1000      |
| F32  | AM                  | -1.50E+00 | -1.39E+00 | -1.39E+00 | -1.22E+00 | -1.50E+00 | -1.21E+00 | -1.31E+00 | -1.40E+00 | -1.16E+00 | -1.17E+00 | -1.44E+00 |
|      | SD                  | 5.90E-11  | 2.32E-01  | 2.22E-01  | 2.97E-01  | 5.90E-11  | 3.10E-01  | 3.18E-01  | 2.13E-01  | 3.19E-01  | 3.06E-01  | 1.74E-01  |
|      | RMSE                | 7.77E-07  | 2.58E-01  | 2.48E-01  | 4.08E-01  | 7.77E-07  | 4.28E-01  | 3.71E-01  | 2.35E-01  | 4.69E-01  | 4.50E-01  | 1.85E-01  |
|      | MAE                 | 7.77E-07  | 1.15E-01  | 1.10E-01  | 2.80E-01  | 7.77E-07  | 2.95E-01  | 1.92E-01  | 9.96E-02  | 3.44E-01  | 3.30E-01  | 6.42E-02  |
|      | Iter <sub>avg</sub> | 1000      | 1000      | 1000      | 1000      | 1000      | 1000      | 1000      | 1000      | 1000      | 1000      | 1000      |
| F33  | AM                  | 0         | 0         | 0         | 0         | 0         | 1.75E-01  | 1.21E-09  | 1.92E-07  | 0         | 6.92E-03  | 0         |
|      | SD                  | 0         | 0         | 0         | 0         | 0         | 1.87E-01  | 1.68E-09  | 1.12E-06  | 0         | 2.40E-02  | 0         |
|      | RMSE                | 0         | 0         | 0         | 0         | 0         | 2.56E-01  | 2.07E-09  | 1.14E-06  | 0         | 2.50E-02  | 0         |
|      | MAE                 | 0         | 0         | 0         | 0         | 0         | 1.75E-01  | 1.21E-09  | 1.92E-07  | 0         | 6.92E-03  | 0         |
|      | Iter <sub>avg</sub> | 88        | 439       | 310       | 1000      | 704       | 1000      | 1000      | 983       | 162       | 1000      | 307       |

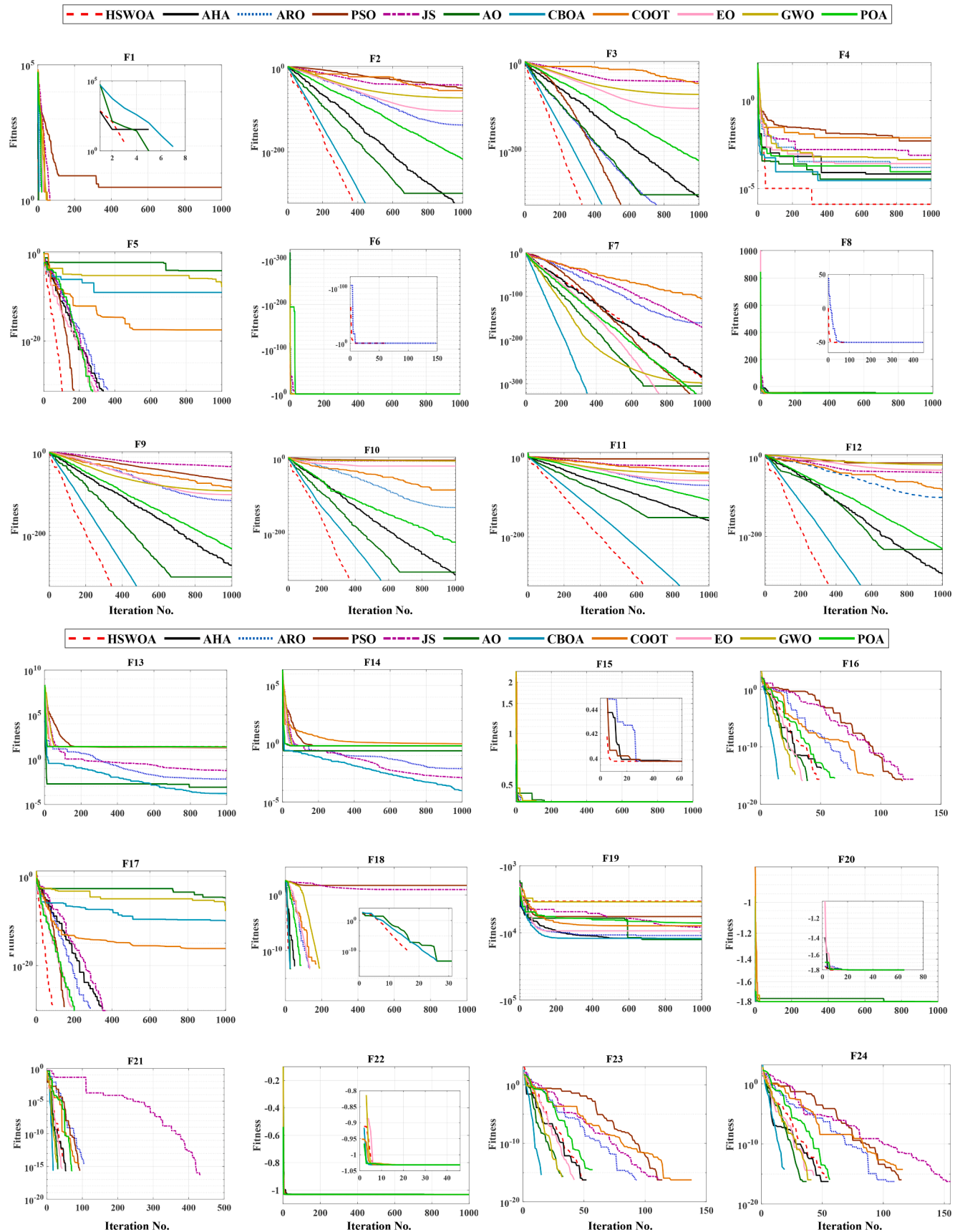


Fig. 4. The convergence curves of HSWOA vs. the comparative techniques.

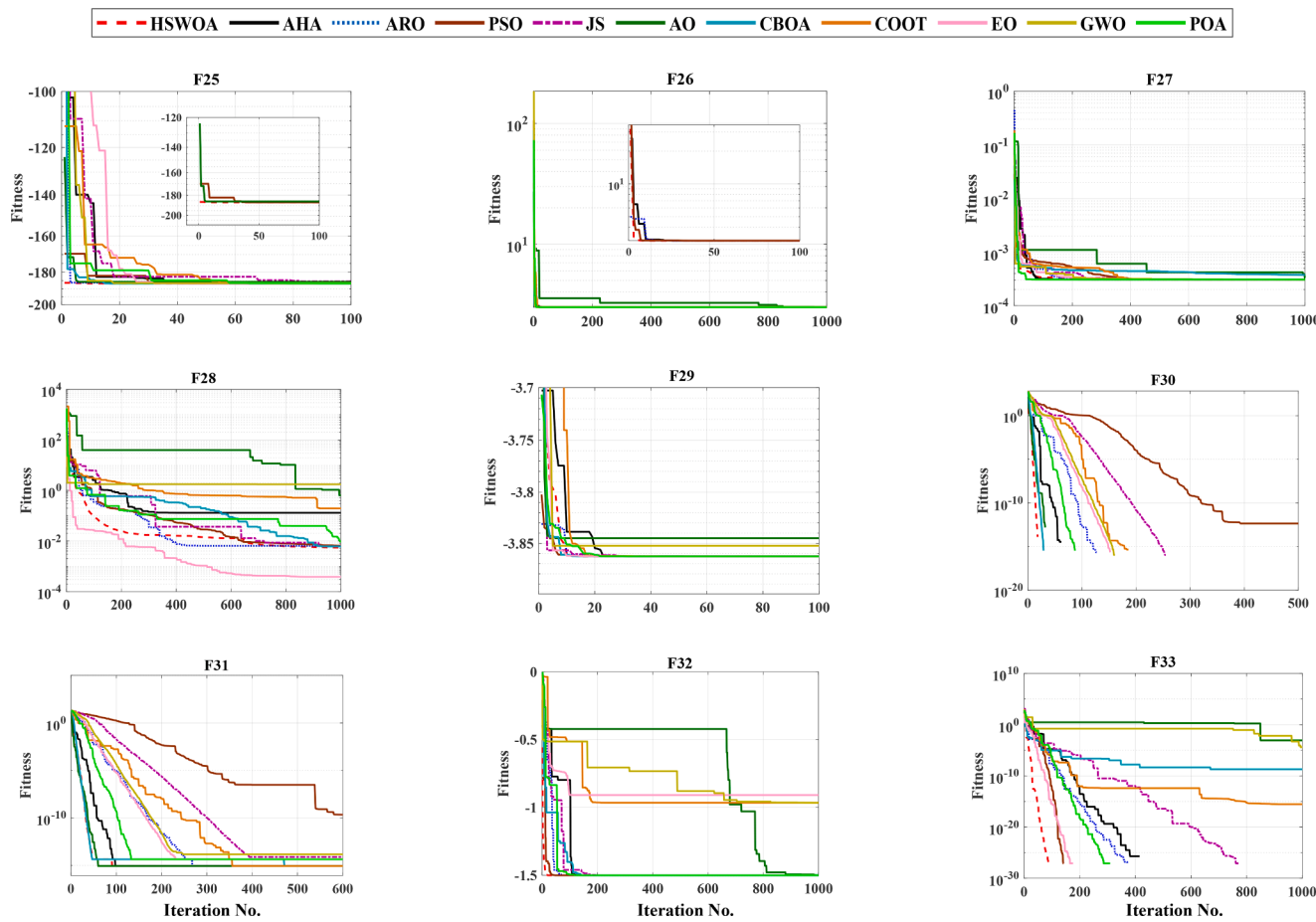


Fig. 4. (continued).

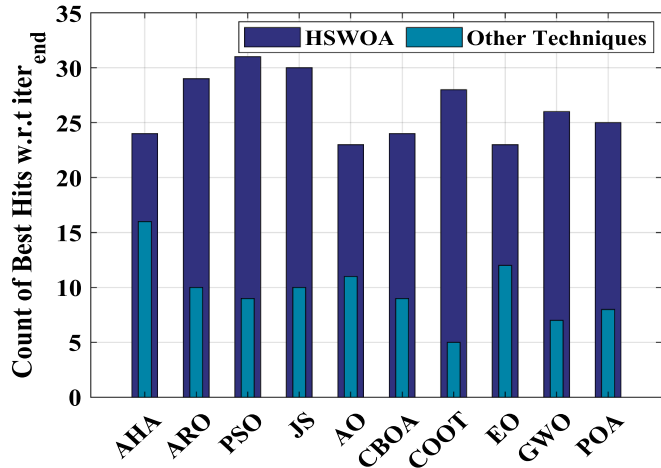


Fig. 5. Count of best hits of HSWOA compared to other techniques.

$$\begin{aligned}
 I_{ph, \text{array}} &= I_{ph} * N_{par}, \text{ and } I_{o, \text{array}} = I_o * N_{par}, \\
 V_{oc, \text{array}}(T) &= V_{oc}(T) * N_{ser}, \\
 I_{sc}(T) &= I_{sc} + K_i * (T_{ak} - T_{rk}), \\
 R_{s, \text{array}} &= R_s * (N_{ser}/N_{par}), \text{ and } R_{sh, \text{array}} = R_{sh} * (N_{ser}/N_{par}).
 \end{aligned}$$

## 5. MPPT of PV array under PSCs using HSWOA

### 5.1. Case study 1

Four Kyocera KD135SX-UPU PV modules are applied to measure the superiority of HSWOA for MPPT of PV array under PSCs. A comprehensive statistical evaluation of HSWOA, GA CS PSO, Harmony Search Algorithm (HSA), Sine Cosine Algorithm (SCA), Differential Evolution algorithm (DE), Wind Driven Optimization algorithm (WDO) and Bat Algorithm (BA) is carried out for two different partial shading scenarios for MPPT of PV array under PSCs by optimizing Eq. (16) over 50 runs.

The proposed technique's results are contrasted with those obtained using previously developed techniques in [26]. There are two different partial shading scenarios as shown in Table 10. The two applied scenarios with GMPP are presented in Fig. 11.

The detailed performance of each optimizer for the two scenarios are illustrated in Fig. 12 and Fig. 13. HSWOA has the best performance over the comparative technique for MPPT under the different shading scenarios in Fig. 12 and Fig. 13. Table 11 provides a summary of the statistical measured performance evaluation for each technique under various shadow scenarios.

From Table 11, it is obvious from the results that HSWOA has highest AM compared to other techniques for the 1st scenario and has nearest value to the best value WDO for the 2nd scenario. For example, in the 1st scenario AM equal (195.77) which are the nearest value compared to the other techniques to the GMPP (196.42).

The MAE varies between 0.6467 and 12.26 for the 1st scenario, the highest value for BA optimizer and the smallest for. The highest value of SD for the 2nd scenario equals 13.71 for PSO optimizer and the lowest

**Table 7**

Statistical results of Wilcoxon signed-rank test for HSWOA versus other optimizers.

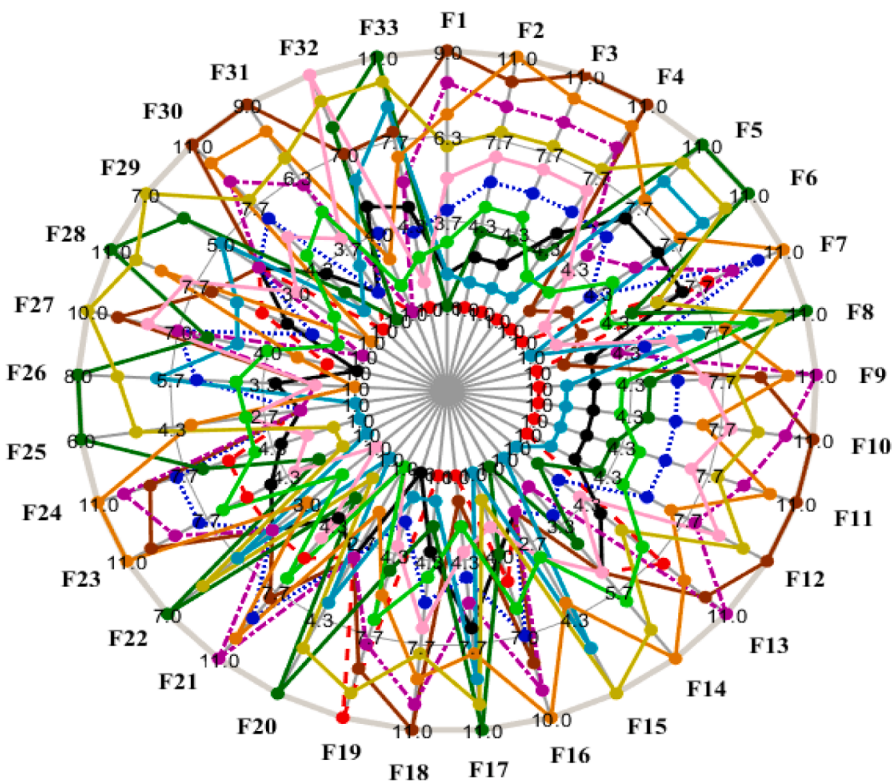
| Function Characteristics | HWSWA vs AHA  | HWSWA vs ARO  | HWSWA vs PSO | HWSWA vs JS  | HWSWA vs AO  |
|--------------------------|---------------|---------------|--------------|--------------|--------------|
| US                       | (+/-/-)       | (+/-/-)       | (+/-/-)      | (+/-/-)      | (+/-/-)      |
| UN                       | (4/0/0)       | (4/0/0)       | (4/0/0)      | (4/0/0)      | (3/1/0)      |
| MS                       | (7/1/2)       | (8/0/2)       | (8/1/1)      | (9/0/1)      | (7/0/3)      |
| MN                       | (2/2/2)       | (3/2/1)       | (3/2/1)      | (3/2/1)      | (3/0/3)      |
| Total                    | (4/4/5)       | (8/4/1)       | (9/4/0)      | (7/5/1)      | (9/0/4)      |
| Function Characteristics | HWSWA vs CBOA | HWSWA vs COOT | HWSWA vs EO  | HWSWA vs GWO | HWSWA vs POA |
| US                       | (+/-/-)       | (+/-/-)       | (+/-/-)      | (+/-/-)      | (+/-/-)      |
| UN                       | (4/0/0)       | (4/0/0)       | (4/0/0)      | (4/0/0)      | (4/0/0)      |
| MS                       | (7/0/3)       | (10/0/0)      | (7/1/2)      | (8/0/2)      | (8/0/2)      |
| MN                       | (4/0/2)       | (4/0/2)       | (3/0/3)      | (4/0/2)      | (4/0/2)      |
| Total                    | (9/0/4)       | (8/0/3)       | (7/1/5)      | (10/0/3)     | (9/0/4)      |
|                          | (24/0/9)      | (28/0/5)      | (21/2/10)    | (26/0/7)     | (25/0/8)     |

**Table 8**

Friedman test of all compared optimizers for 33 functions.

|               | HWSWA | AHA  | ARO   | PSO   | JS    | AO    | CBOA  | COOT  | EO    | GWO   | POA   |
|---------------|-------|------|-------|-------|-------|-------|-------|-------|-------|-------|-------|
| Sum of ranks  | 147.5 | 148  | 171   | 261.5 | 216.5 | 203.5 | 151.5 | 268.5 | 206.5 | 262.5 | 181   |
| Mean of ranks | 8.61  | 8.71 | 10.06 | 15.38 | 12.74 | 11.97 | 8.91  | 15.79 | 12.15 | 15.44 | 10.65 |
| Overall ranks | 1     | 2    | 4     | 9     | 8     | 6     | 3     | 11    | 7     | 10    | 5     |

— HSWOA — AHA ..... ARO — PSO — JS — AO — CBOA — COOT — EO — GWO — POA

**Fig 6.** Radar chart for ranks among all compared algorithms.

value equals 1.7467 for HSWOA. For RMSE, 16.76 is the highest value for BA algorithm, and 1.8088 is the lowest value for HSWOA.

## 5.2. Case study 2

Five tata power solar systems TP250MBZ modules are used to discuss the conditions of partial shading and its specifications are showed in Appendix C.

Two various shading scenarios are taken into consideration. The purpose of altering the shading models is to relocate the global MPP from the left to the right or center in order to measure the reaction of HSWOA with various examples demonstrating its consistent quality for monitoring the GMPP. Two various PVs formations are taken into account: the first has five series-connected PV panels, while the second has five. According to Table 12, there are two distinct partial shading scenarios. The results of HSWOA are compared with PSO and (CS)

**Table 9**

Results of CEC2019 functions for all compared optimizers.

| Fun. | Index | HWSOA    | AHA      | ARO      | PSO      | JS       | AO       | CBOA     | COOT     | EO       | GWO        | POA      |
|------|-------|----------|----------|----------|----------|----------|----------|----------|----------|----------|------------|----------|
| CF1  | AM    | 3.64E+01 | 3.53E+01 | 2.78E+01 | 1.78E+01 | 3.35E+01 | 1.79E+02 | 4.45E+02 | 5.50E+01 | 1.14E+01 | 1.38E+02   | 3.93E+02 |
|      | SD    | 2.52E+01 | 2.06E+01 | 1.17E+01 | 6.89E+00 | 2.18E+01 | 1.19E+02 | 2.31E+02 | 2.47E+01 | 5.09E+00 | 4.04E+02   | 7.93E+02 |
| CF2  | AM    | 2.11E+00 | 2.08E+00 | 2.08E+00 | 2.13E+00 | 2.04E+00 | 2.31E+00 | 2.19E+00 | 2.08E+00 | 2.05E+00 | 2.38E+00   | 2.36E+00 |
|      | SD    | 6.84E-02 | 5.48E-02 | 4.96E-02 | 2.13E+00 | 2.25E-02 | 1.20E-01 | 1.05E-01 | 4.87E-02 | 3.76E-02 | 2.22E-01   | 1.95E-01 |
| CF3  | AM    | 4.10E+00 | 3.80E+00 | 3.90E+00 | 4.62E+00 | 2.99E+00 | 4.80E+00 | 3.85E+00 | 4.88E+00 | 2.96E+00 | 4.49519879 | 3.90E+00 |
|      | SD    | 1.11E+00 | 7.67E-01 | 6.31E-01 | 8.75E-01 | 8.77E-01 | 5.85E-01 | 5.06E-01 | 7.14E-01 | 1.13E+00 | 0.96264191 | 5.82E-01 |
| CF4  | AM    | 3.35E+00 | 3.41E+00 | 3.41E+00 | 3.35E+00 | 3.36E+00 | 4.75E+00 | 5.38E+00 | 3.47E+00 | 3.35E+00 | 4.92E+00   | 7.32E+00 |
|      | SD    | 5.54E-03 | 6.15E-02 | 5.32E-02 | 8.31E-03 | 1.15E-02 | 6.83E-01 | 5.60E-01 | 5.90E-02 | 3.97E-03 | 7.49E-01   | 1.25E+01 |
| CF5  | AM    | 1.81E+01 | 1.79E+01 | 1.78E+01 | 2.10E+01 | 1.70E+01 | 1.78E+01 | 1.81E+01 | 1.93E+01 | 2.04E+01 | 2.14E+01   | 1.86E+01 |
|      | SD    | 7.26E+00 | 7.04E+00 | 7.27E+00 | 6.06E-02 | 7.13E+00 | 7.07E+00 | 5.72E+00 | 5.78E+00 | 3.61E+00 | 8.81E-02   | 5.67E+00 |

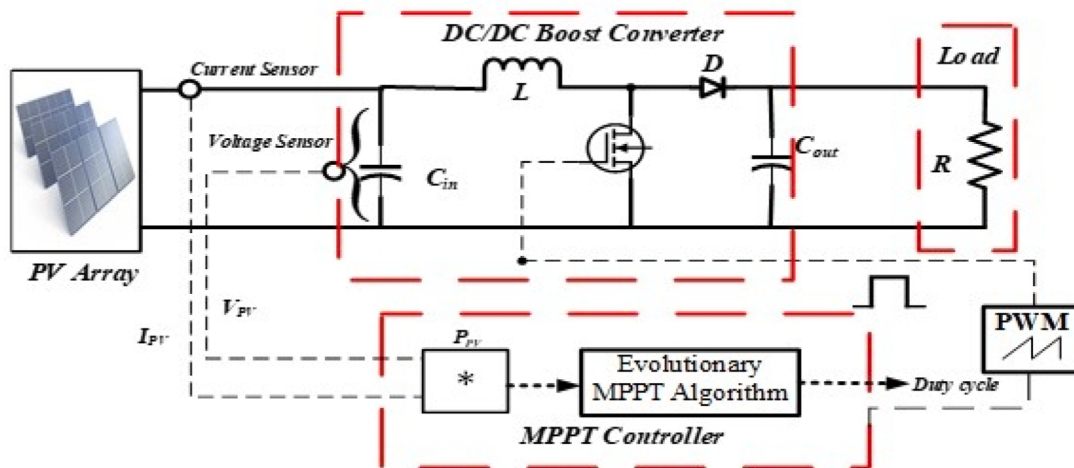


Fig. 7. Circuit diagram of a PV generating system.

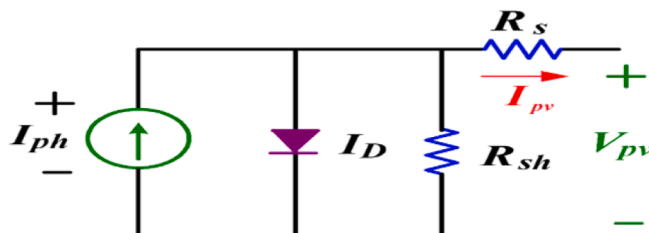


Fig. 8. Single-diode model of PV module.

algorithm to measure the validity of it by applying them to the system in Fig. 7. The comparison is based on measuring the average power capturing factor (APCF) of each technique. The one has the highest APCF; it will be more efficient one than others.

$$APCF = \frac{\sum_{t=0}^T P_{pv} * \Delta t}{T_s * P_{GMPP}} \times 100\% \quad (21)$$

where  $P_{pv}$  is the instantaneous PV array power,  $\Delta t$  is the sample time (6  $\mu s$ ),  $T_s$  is the simulation time (2 sec),  $P_{GMPP}$  is the global power of PV array.

The two scenarios with GMPP are shown in Fig. 14. The solar

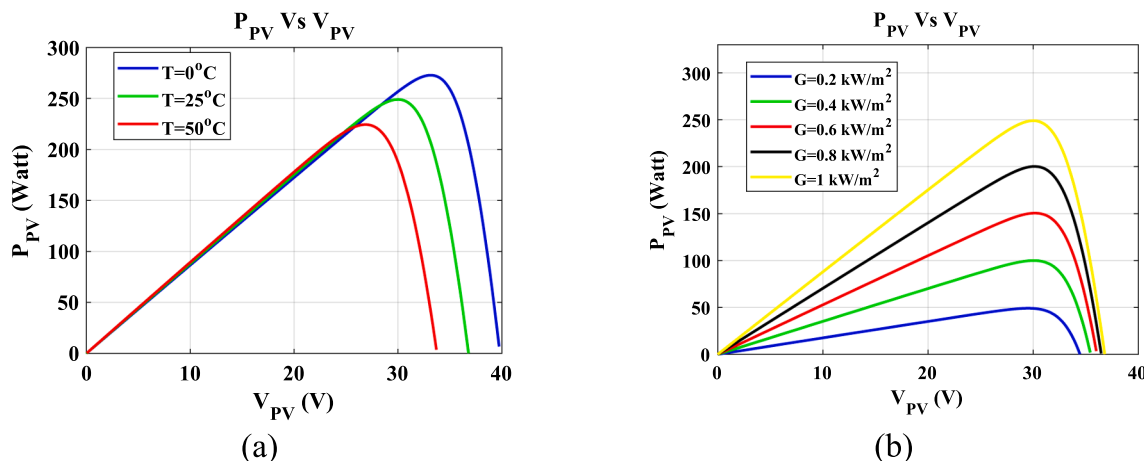


Fig. 9. P-V characteristics graph for (a) various temperature levels, (b) different irradiation levels.

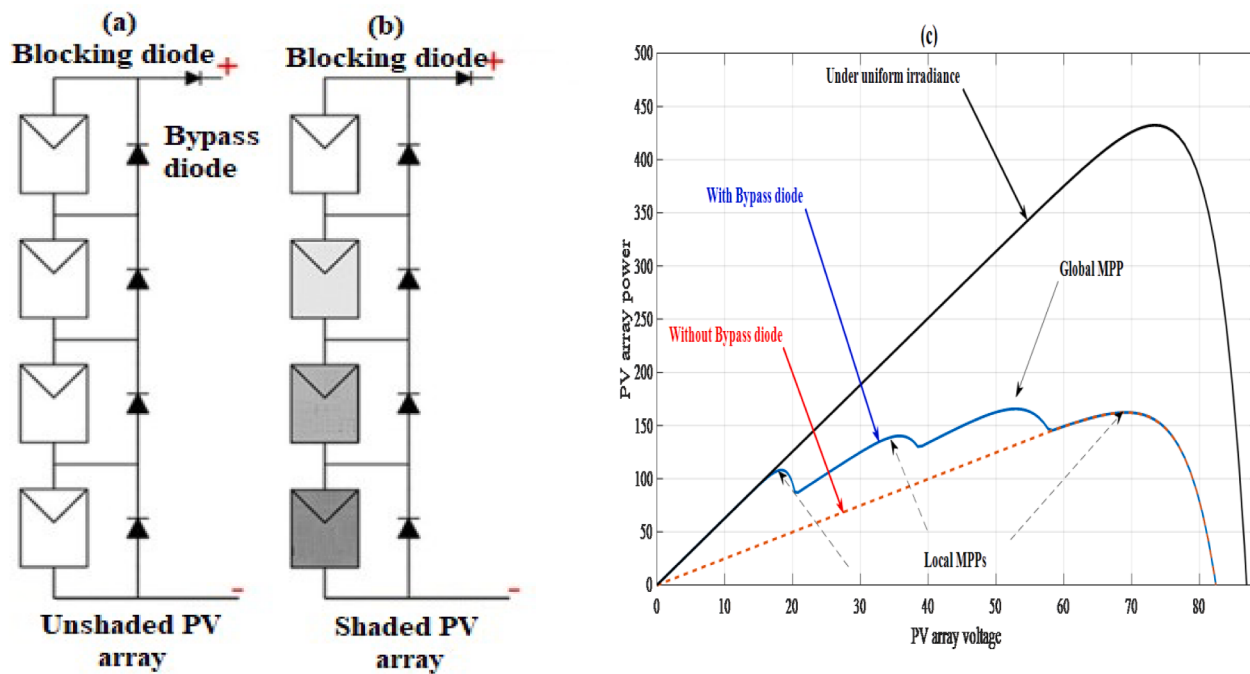


Fig. 10. (a) Unshaded PV array. (b) Shaded PV array. (c) PV characteristics of PV array under different conditions.

Table 10

The PV array with different shading scenarios.

|              | PV array structure | Solar irradiance Levels distribution on modules | Power at MPP, W | Position of GMPP |
|--------------|--------------------|---|-----------------|------------------|
| 1st Scenario | Four modules       | 900,700,400,200                                 | 196.42          | 2nd left         |
| 2nd Scenario | Four modules       | 1000,800,600,400                                | 255.64          | 2nd right        |

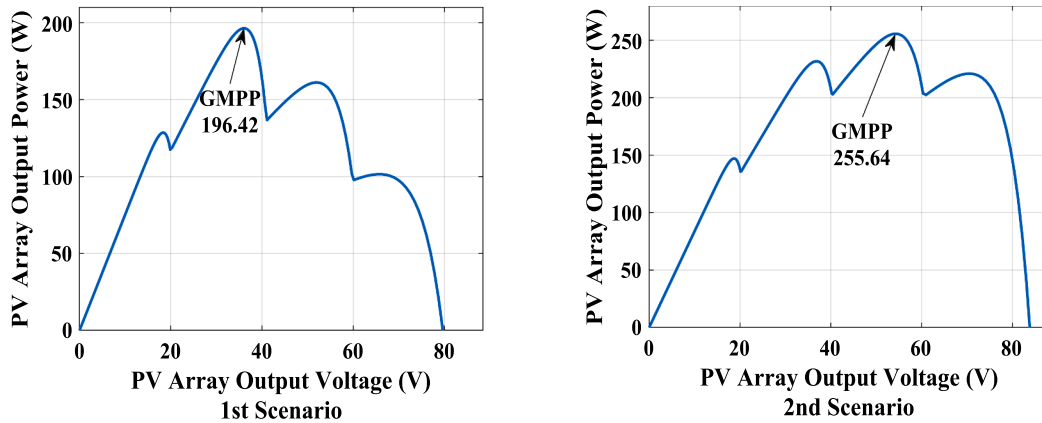


Fig. 11. The P-V curves of the proposed PV array with distinct shading scenarios.

radiation levels of 500, 800, 900, 1000 W/m<sup>2</sup> are applied to first, second, third and fourth PV modules respectively in the first scenario. While the second scenario is illustrated in the figure.

Fig. 15 shows the curve of PV array power ( $P_{PV}$ ), for the 1st scenario and 2nd scenario. In the 1st scenario four modules subjected to high irradiance levels as shown in Table 12 so, all techniques present a good performance for tracking MPP but HSWOA present a slightly closed performance to GMPP with a APCF 98.57% which is higher than that one of CS by percentage 2.21% and that one of PSO by percentage 6.12% as shown in Table 13. In addition to that, the lowest tracking time for GMPP is 0.4514 s for HSWOA and the highest one is 1.162 s for PSO.

In the 2nd scenario, most difficult conditions are provided where the number of PV modules is increased to be five modules with low irradiance levels as shown in Table 12. In this scenario, HSWOA presents a superior performance for tracking GMPP over all comparative techniques with a APCF 98.04% which is higher than that one of CS by percentage 4.98% and that one of PSO by percentage 13.7% as shown in Table 13. Also, the lowest tracking time for GMPP is 0.4521 s for HSWOA and the highest one is 1.171 s for PSO.

According to Worldwide weather forecasts and climate information website, the average annual amount of sun in Cairo is 3450 h. Therefore, HSWOA presents energy saving about 960.258 kWh, while CS and PSO

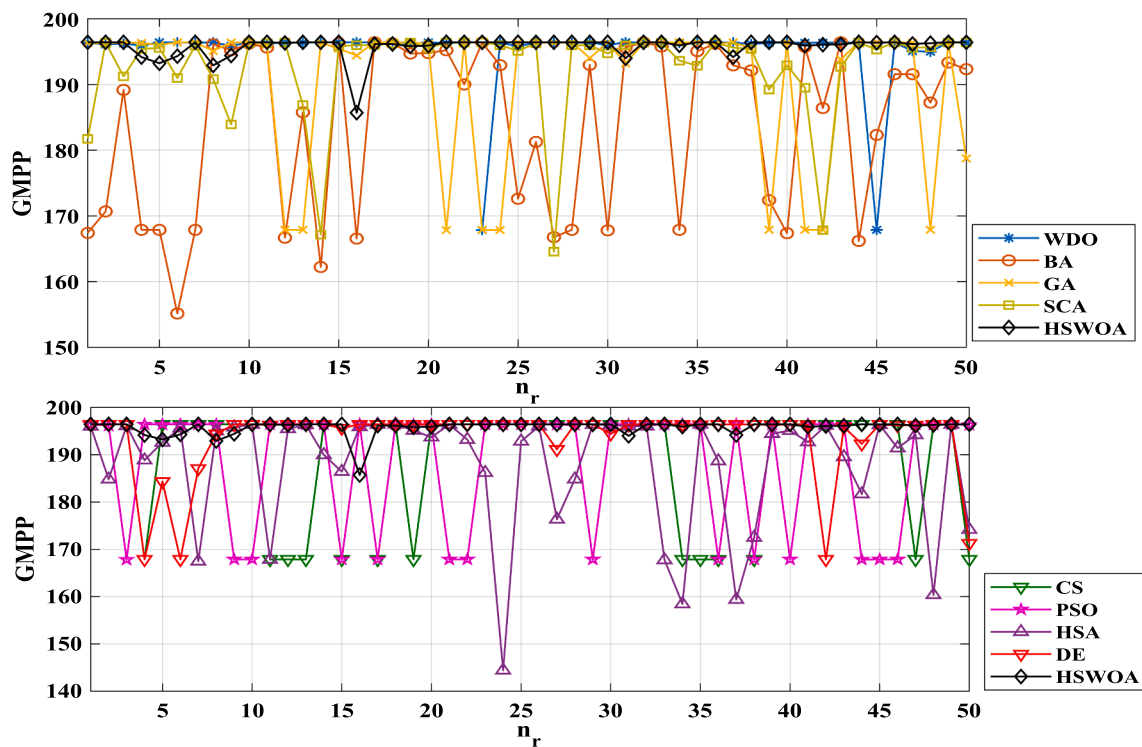


Fig. 12. The detailed performance of each technique for the 1st shading scenario.

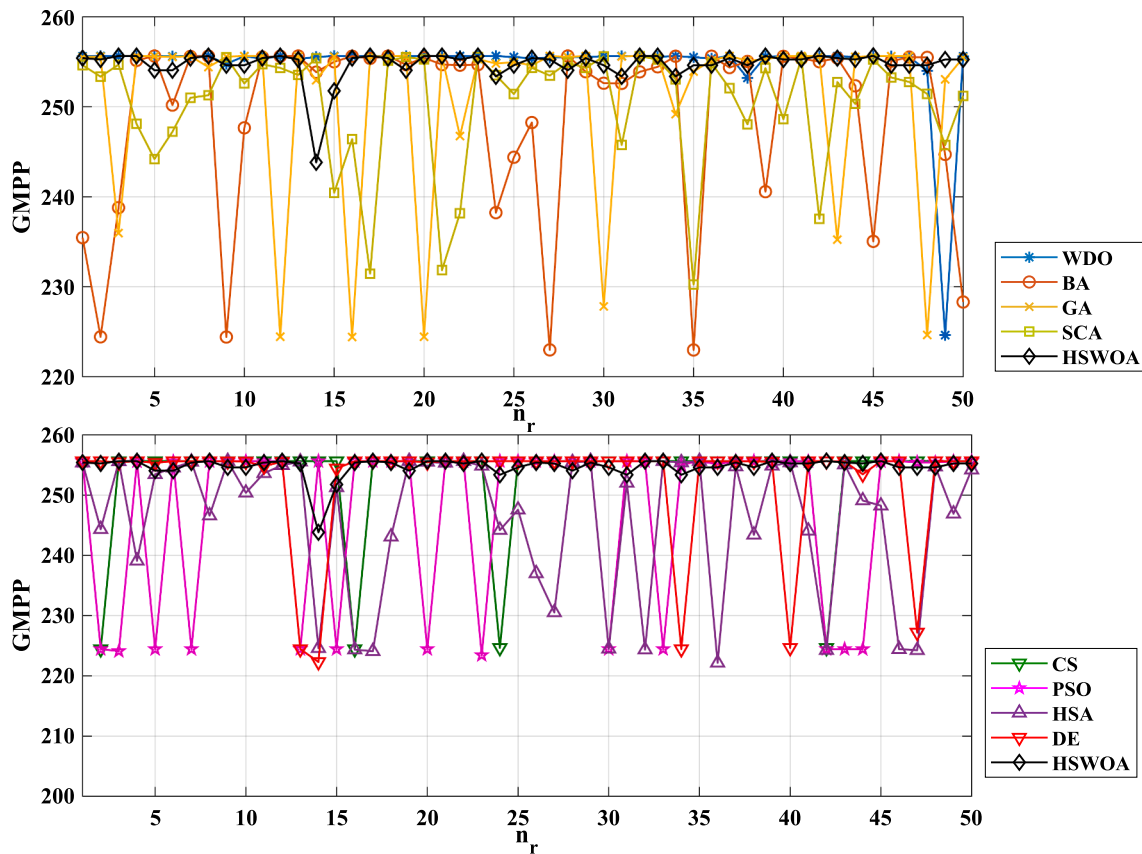


Fig. 13. The detailed performance of each optimizer for the 2nd shading scenario.

**Table 11**

Evaluation of statistical performance of the optimizers for different shading scenarios.

| Algorithm   | DE     | HAS    | PSO    | CS     | SCA    | GA     | Bat    | WDO           | HWOA          |
|---|--------|--------|--------|--------|--------|--------|--------|---------------|---------------|
| <i>Arithmetic Mean of the optimum solution (AM)</i> |        |        |        |        |        |        |        |               |               |
| 1st scenario  | 193.46 | 187.66 | 188.41 | 189    | 192.71 | 190.62 | 184.15 | 195.13        | <b>195.77</b> |
| 2nd scenario  | 252.43 | 246.26 | 247.47 | 253.15 | 250.43 | 251.21 | 249.37 | <b>254.87</b> | 254.75        |
| <i>RMSE</i>   |        |        |        |        |        |        |        |               |               |
| 1st scenario  | 8.19   | 15.33  | 15.1   | 14.55  | 8.24   | 12.39  | 17.76  | 5.72          | <b>1.8088</b> |
| 2nd scenario  | 9.83   | 15.01  | 15.96  | 9.82   | 8.38   | 10.58  | 11.76  | 4.41          | <b>1.9606</b> |
| <i>MAE</i>  |        |        |        |        |        |        |        |               |               |
| 1st scenario  | 2.88   | 8.76   | 8.01   | 7.42   | 3.7    | 5.8    | 12.26  | 1.28          | <b>0.6467</b> |
| 2nd scenario  | 3.21   | 9.37   | 8.17   | 3.11   | 5.21   | 4.43   | 6.27   | <b>0.77</b>   | 0.8905        |
| <i>SD</i>   |        |        |        |        |        |        |        |               |               |
| 1st scenario  | 7.67   | 12.58  | 12.81  | 12.52  | 7.36   | 10.95  | 12.85  | 5.57          | <b>1.6893</b> |
| 2nd scenario  | 9.29   | 11.73  | 13.71  | 9.32   | 5.56   | 9.61   | 9.95   | 4.34          | <b>1.7467</b> |

**Table 12**

The PV array with different shading scenarios.

|              | PV array structure | Solar irradiance Levels distribution on modules | Power at MPP, W | Position of GMPP |
|--------------|--------------------|---|-----------------|------------------|
| 1st Scenario | Four modules       | 500,800,900,1000                                | 635.4           | 2nd right        |
| 2nd Scenario | Five modules       | 300,550,250,600,100                             | 283.9           | 2nd left         |

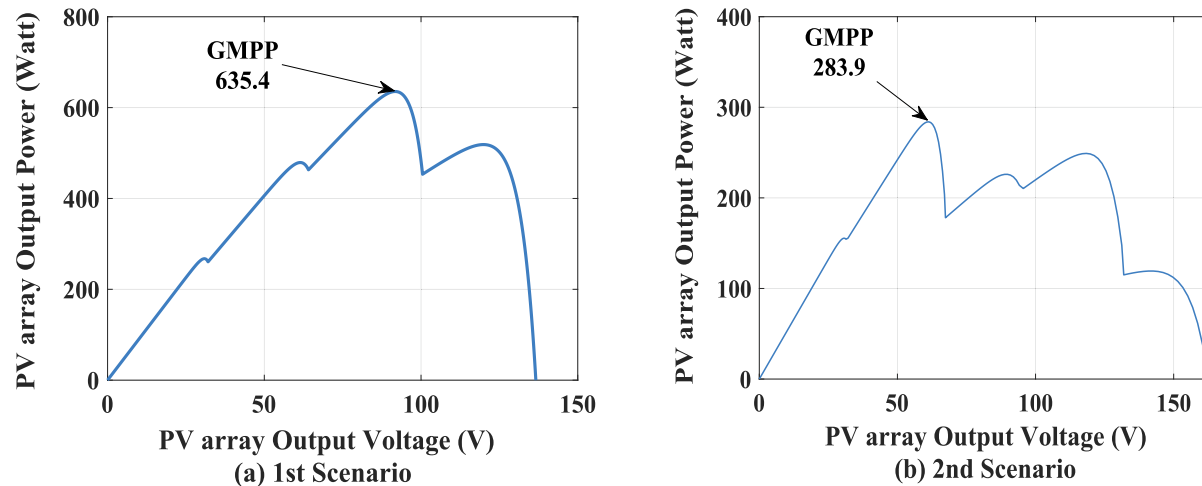


Fig. 14. The P-V curves of the studied PV array with different shading scenarios.

are about 911.481 kWh and 826.072 kWh, respectively for the worst-case scenario (cloudy days). For the other scenario (sunny days), HSWOA achieves energy power saving about 2160.783 kWh, while CS and PSO are about 2112.336 kWh and 2026.624 kWh.

## 6. Conclusions future works

A novel bioinspired optimization method, namely the Harbor Seal Whiskers Optimization Algorithm (HSWOA), inspired from the high sensing ability of seal whiskers in tracking its prey, was proposed for transacting with various optimization tasks in this work. Two sets of numerical test functions: 33 benchmark functions and five CEC2019 benchmark functions were applied to examine the effectiveness of the HSWOA. The results showed that HSWOA could identify the global maximum optimum in comparison to other comparative optimizers.

Further, the results demonstrated HSWOA's superiority and achievement in terms of computational demands and solution accuracy. HSWOA hit the optimal solution of 23 benchmark functions out of 35 which was the highest number compared with the comparative techniques with a smaller number of iterations with small errors and standard deviation. Eventually, HSWOA was employed to track maximum power point of PV array under PSCs for two case studies. The 1st case study is applied to two scenarios. The results of this case show that the reliability and superiority of HSWOA over the comparative. The results of the 2nd case study showed a best performance for tracking the global maximum power point with best average power capturing factor of 98.57% in minimum tracking time of 0.4514 s. HSWOA was shown to provide annual energy saving by about 1 MWh for cloudy days (five modules) and 2 MWh for sunny days (four modules). Future work toward calculating the main parameters of the proposed technique using suitable

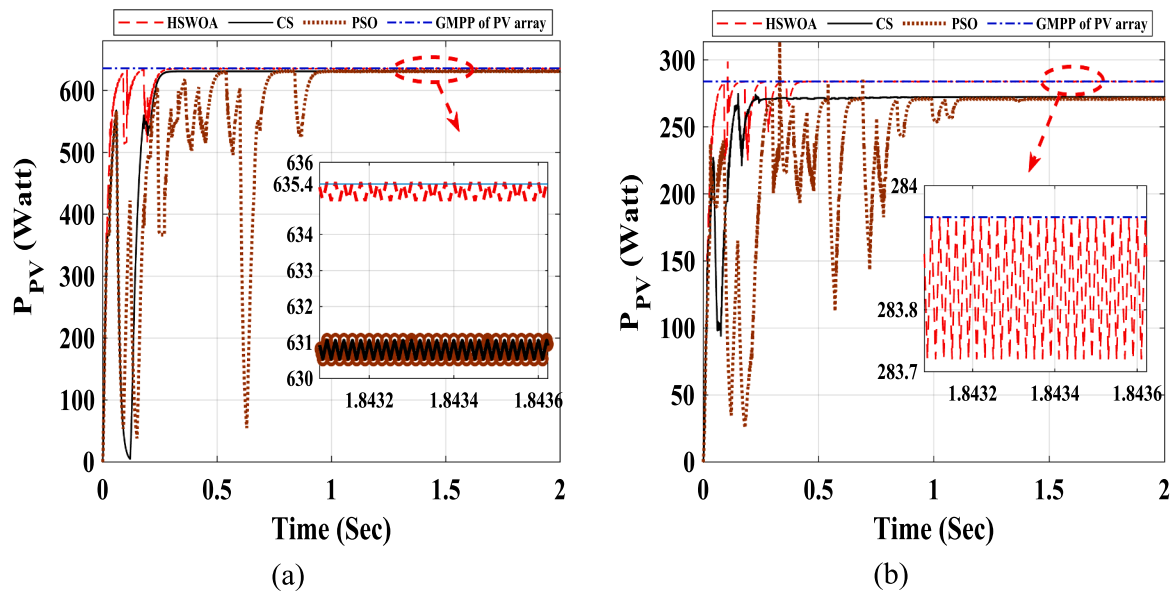


**Fig. 15.** The performance curve of PV array power ( $P_{PV}$ ), for (a) 1st scenario and for (b) 2nd scenario.

**Table 13**  
Performance analysis of the PV system at the different cases studies.

| Algorithm             | HSWOA  |        | CS     |        | PSO    |       |
|-----------------------|--------|--------|--------|--------|--------|-------|
| Performance Parameter | APCF   | TT     | APCF   | TT     | APCF   | TT    |
| 1st scenario          | 98.57% | 0.4514 | 96.36% | 0.8147 | 92.45% | 1.162 |
| 2nd scenario          | 98.04% | 0.4521 | 93.06% | 0.8699 | 84.34% | 1.171 |

optimization technique would be carried out instead of using trial and

#### Appendix A. . 33 benchmark functions used in test 1

A.1. Benchmark functions, C: Characteristics, Dim: Dimensions, U: Unimodal, S: Separable, M: Multimodal, N: Non-separable

| Name          | Function   | C  | Range        | Dim | $f_{opt}$ |
|---------------|--|----|--------------|-----|-----------|
| Step          | $f_1(x) = \sum_{i=1}^{30} (\lfloor x_i + 0.5 \rfloor)^2$   | US | [-100,100]   | 30  | 0         |
| Sphere        | $f_2(x) = \sum_{i=1}^{30} x_i^2$   | US | [-100,100]   | 30  | 0         |
| SumSquares    | $f_3(x) = \sum_{i=1}^{30} i x_i^2$   | US | [-10,10]     | 30  | 0         |
| Quartic       | $f_4(x) = \sum_{i=1}^{30} i x_i^4 + \text{random}[0, 1]$   | US | [-1.28,1.28] | 30  | 0         |
| Beale         | $f_5(x) = (1.5 - x_1 + x_1 x_2)^2 + (2.25 - x_1 + x_1 x_2^2)^2 + (2.625 - x_1 + x_1 x_2^3)^2$  | UN | [-4.5,4.5]   | 2   | 0         |
| Easom         | $f_6(x) = -\cos(x_1)\cos(x_2)\exp[-(x_1 - \pi)^2 - (x_2 - \pi)^2]$   | UN | [-100,100]   | 2   | -1        |
| Matyas        | $f_7(x) = 0.26(x_1^2 + x_2^2) - 0.48x_1x_2$  | UN | [-10,10]     | 2   | 0         |
| Trid6         | $f_8(x) = \sum_{i=1}^6 (x_i - 1)^2 - \sum_{i=2}^6 x_i x_{i-1}$   | UN | [-6^2,6^2]   | 6   | -50       |
| Zakharov      | $f_9(x) = \sum_{i=1}^{10} x_i^2 + \left(\sum_{i=1}^{10} 0.5ix_i\right)^2 + \left(\sum_{i=1}^{10} 0.5ix_i\right)^4$                   | UN | [-5,10]      | 10  | 0         |
| Powell        | $f_{10}(x) = \sum_{i=1}^{24} (x_{4i-3} + 10x_{4i-2})^2 + 5(x_{4i-1} - x_{4i})^2 + (x_{4i-2} - x_{4i-1})^2 + 10(x_{4i-3} - x_{4i})^2$ | UN | [-4,5]       | 24  | 0         |
| Schwefel 2.22 | $f_{11}(x) =  x_1  + \prod_{i=2}^{30}  x_i $   | UN | [-10,10]     | 30  | 0         |
| Schwefel 1.2  | $f_{12}(x) = \sum_{i=1}^{30} \left(\sum_{j=1}^i x_j\right)^2$  | UN | [-100,100]   | 30  | 0         |
| Rosenbrock    | $f_{13}(x) = \sum_{i=1}^{29} \left(100(x_{i+1} - x_i^2)^2 + (x_i - 1)^2\right)$  | UN | [-30,30]     | 30  | 0         |
| Dixon-Price   | $f_{14}(x) = (x_1 - 1)^2 + \sum_{i=2}^{30} i(2x_i^2 - x_{i-1})^2$  | UN | [-10,10]     | 30  | 0         |

A.2. Benchmark functions, C: Characteristics, Dim: Dimensions, U: Unimodal, S: Separable, M: Multimodal, N: Non-separable.

| Name                       | Function  | C  | Range            | Dim | $f_{opt}$ |
|----------------------------|---|----|------------------|-----|-----------|
| <b>Branin</b>              | $f_{15}(x) = \left(x_2 - \frac{5.1x_1^2}{4\pi^2} + \frac{5x_1}{\pi} - 6\right)^2 + 10\left(1 - \frac{1}{8\pi}\right)\cos(x_1) + 10$   | MS | [-5,10] × [0,15] | 2   | 0.398     |
| <b>Bohachevsky1</b>        | $F_{16}(x) = x_1^2 + 2x_2^2 - 0.3\cos(3\pi x_1) - 0.4\cos(4\pi x_2) + 0.7$  | MS | [-100,100]       | 2   | 0         |
| <b>Booth</b>               | $f_{17}(x) = (x_1 + 2x_2 - 7)^2 + (2x_1 + x_2 - 5)^2$   | MS | [-10,10]         | 30  | 0         |
| <b>Rastrigin</b>           | $f_{18}(x) = 10Dim + \sum_{i=1}^{30} (x_i^2 - 10\cos(2\pi x_i))$  | MS | [-5.12,5.12]     | 30  | 0         |
| <b>Schwefel</b>            | $f_{19}(x) = \sum_{i=1}^{30} -x_i \sin(\sqrt{ x_i })$   | MS | [-500,500]       | 30  | -12,569.5 |
| <b>Michalewicz2</b>        | $f_{20}(x) = -\sum_{i=1}^2 \sin(x_i) \sin^{20}\left(\frac{i\pi x_i^2}{\pi}\right)$  | MS | [0,π]            | 2   | -1.8013   |
| <b>Schaffer</b>            | $f_{21}(x) = 0.5 + \frac{\sin^2(x_1^2 - x_2^2) - 0.5}{[1 + 0.001(x_1^2 + x_2^2)]^2}$  | MN | [-100,100]       | 2   | 0         |
| <b>Six Hump Camel Back</b> | $f_{22}(x) = \left(4 - 2.1x_1^2 + \frac{x_1^4}{3}\right)x_1^2 + x_1 x_2 + (-4 + 4x_2^2)x_2^2$   | MN | [-5,5]           | 2   | -1.03163  |
| <b>Bohachevsky2</b>        | $f_{23}(x) = x_1^2 + 2x_2^2 - 0.3\cos(3\pi x_1)\cos(4\pi x_2) + 0.3$  | MN | [-100,100]       | 2   | 0         |
| <b>Bohachevsky3</b>        | $f_{24}(x) = x_1^2 + 2x_2^2 - 0.3\cos(3\pi x_1 + 4\pi x_2) + 0.3$   | MN | [-100,100]       | 2   | 0         |
| <b>Shubert</b>             | $f_{25}(x) = \left(\sum_{i=1}^5 i\cos((i+1)x_1 + i)\right)\left(\sum_{i=1}^5 i\cos((i+1)x_2 + i)\right)$  | MN | [-10,10]         | 2   | -186.73   |
| <b>GoldStein-Price</b>     | $f_{26}(x) = f_1(x) + f_2(x)$<br>$f_1(x) = (1 + (x_1 + x_2 + 1)^2(19 - 14x_1 + 3x_1^2 - 14x_2 + 6x_1 x_2 + 3x_2^2))$<br>$f_2(x) = (30 + (2x_1 - 3x_2)^2(18 - 32x_1 + 12x_1^2 + 48x_2 - 36x_1 x_2 + 27x_2^2))$   | MN | [-2,2]           | 2   | 3         |
| <b>Kowalik</b>             | $f_{27}(x) = \sum_{i=1}^{11} \left[ a_i - \frac{x_1(b_i^2 + b_i x_2)}{b_i^2 + b_i x_3 + x_4} \right]^2$<br>$a = [0.19570, 1.9470, 1.7350, 1.60, 0.08440, 0.06270, 0.04560, 0.03420, 0.03230, 0.02350, 0.0246]$<br>$b = \frac{1}{[0.250, 51246810121416]}$ | MN | [-5,5]           | 4   | 0.00031   |
| <b>Perm</b>                | $f_{28}(x) = \sum_{i=1}^4 \left( \sum_{j=1}^4 (j^i + 0.5) \left( \left( \frac{x_j}{j} \right)^i - 1 \right) \right)^2$  | MN | [-4,4]           | 4   | 0         |

A.3. Benchmark functions, C: Characteristics, Dim: Dimensions, U: Unimodal, S: Separable, M: Multimodal, N: Non-separable.

| Name                    | Function   | C  | Range      | Dim | $f_{opt}$ |
|-------------------------|--|----|------------|-----|-----------|
| <b>Hartman3</b>         | $f_{29}(x) = -\sum_{i=1}^4 a_i e^{-\sum_{j=1}^3 A_{ij}(x_j - p_{ij})^2}$<br>$\alpha = (1, 1.2, 3, 3.2)^T$<br>$A = \begin{pmatrix} 3 & 10 & 30 \\ 0.1 & 10 & 35 \\ 3 & 10 & 30 \\ 0.1 & 10 & 35 \end{pmatrix}$<br>$P = 10^{-4} \begin{pmatrix} 3689 & 1170 & 2673 \\ 4699 & 4387 & 7470 \\ 1091 & 8732 & 5547 \\ 381 & 5743 & 8828 \end{pmatrix}$ | MN | [0,1]      | 3   | -3.86     |
| <b>Griewank</b>         | $f_{30}(x) = \frac{1}{4000} \sum_{i=1}^{30} x_i^2 - \prod_{i=1}^{30} \cos\left(\frac{x_i}{\sqrt{i}}\right) + 1$  | MN | [-600,600] | 30  | 0         |
| <b>Ackley</b>           | $f_{31}(x) = -20 e^{-0.2 \times \sqrt{\frac{1}{n} \sum_{i=1}^{30} x_i^2}} - e^{\frac{1}{n} \sum_{i=1}^{30} \cos(2\pi x_i)} + 20 + e^{(1)}$   | MN | [-32,32]   | 30  | 0         |
| <b>Langermann5</b>      | $f_{32}(x) = \sum_{i=1}^5 c_i e^{-\left(\frac{1}{\pi} \sum_{j=1}^5 (x_j - A_{ij})^2\right)} \cos\left(\pi \sum_{j=1}^5 (x_j - A_{ij})^2\right)$  | MN | [0,10]     | 5   | -1.5      |
| <b>Fletcher Powell2</b> | $f_{33}(x) = \sum_{i=1}^n (A_i - B_i)^2$<br>$A_i = \sum_{j=1}^n (a_{ij} \sin a_j + b_{ij} \cos a_j)$<br>$B_i = \sum_{j=1}^n (a_{ij} \sin x_j + b_{ij} \cos x_j)$   | MN | [-π, π]    | 2   | 0         |

#### Appendix B. . CEC 2019 benchmark functions used in test 2 [73]

| Function | Name                            | Range      | Dim | $f_{min}$ |
|----------|---------------------------------|------------|-----|-----------|
| CEC01    | Rastrigin's Function            | [-100,100] | 10  | 1         |
| CEC02    | Griewank's Function             | [-100,100] | 10  | 1         |
| CEC03    | Expanded Schaffer's F6 Function | [-100,100] | 10  | 1         |
| CEC04    | Happy Cat Function              | [-100,100] | 10  | 1         |
| CEC05    | Ackley Function                 | [-100,100] | 10  | 1         |

## Appendix C. . PV module specifications of Tata Power Solar Systems TP250MBZ module

| Type   | Tata Power Solar Systems TP250MBZ                 |
|--|---|
| Maximum power, $P_{max}$                             | 249 W   |
| Open circuit voltage, $V_{oc}$                       | 36.8 V  |
| Voltage at maximum power point                       | 30 V  |
| Short circuit current, $I_{sc}$                      | 8.83 A  |
| Current at maximum power point                       | 8.3 A   |
| Short circuit current temperature coefficient, $K_i$ | $63.81 \times 10^{-3} \text{ A/}^{\circ}\text{C}$ |
| Open circuit voltage temperature coefficient, $K_v$  | $-3 \times 10^{-2} \text{ V/}^{\circ}\text{C}$    |
| Reference temperature, $T_{ref}$                     | 25 °C   |

## References

- [1] D.K. Sarmah, A.J. Kulkarni, A. Abraham, Optimization models in steganography using metaheuristics, Springer International Publishing, 2020.
- [2] R. Silhavy (Ed.), Artificial Intelligence and Bioinspired Computational Methods: Proceedings of the 9th Computer Science On-line Conference, Springer Nature, 2020, p. 2.
- [3] H. Malik, A. Iqbal, P. Joshi, S. Agrawal, I.F. Bakhsh, et al., Metaheuristic and evolutionary computation: algorithms and applications, Springer, Berlin/Heidelberg, Germany, 2021.
- [4] H. Malik, A. Iqbal, P. Joshi, S. Agrawal, et al., Metaheuristic and evolutionary computation: algorithms and applications, Springer Nature Singapore, 2021.
- [5] E.G. Talbi, Metaheuristics: from design to implementation, John Wiley & Sons, 2009.
- [6] H.M. Sultan, A.S. Menes, S. Kamel, A. Korashy, S.A. Almohaimeed, M. Abdel-Akher, An improved artificial ecosystem optimization algorithm for optimal configuration of a hybrid PV/WT/FC energy system, *Alex. Eng. J. (Elsevier)*. 60 (1) (2021) 1001–1025.
- [7] J.K. Mandal, S.C. Satapathy, M.K. Sanyal, et al., Information systems design and intelligent applications: proceedings of second international conference INDIA 2015, Volume 2. Springer India, New Delhi, 2015.
- [8] X. Yue, H. Zhang, Improved hybrid bat algorithm with invasive weed and its application in image segmentation, *Arab. J. Sci. Eng.* 44 (11) (2019) 9221–9234.
- [9] D. Yoursi, T.S. Babu, D. Allam, V.K. Ramachandaramurthy, M.B. Etiba, A novel chaotic flower pollination algorithm for global maximum power point tracking for photovoltaic system under partial shading conditions, *IEEE Access* 7 (2019) 121432–121445.
- [10] A.M. Kamoona, J.C. Patra, A. Stojcevski, An enhanced cuckoo search algorithm for solving optimization problems, in: 2018 IEEE Congress on Evolutionary Computation (CEC). IEEE, 2018, 1–6.
- [11] A. Iglesias, A. Gálvez, P. Suárez, M. Shinya, N. Yoshida, C. Otero, C. Manchado, V. Gomez-Jauregui, Cuckoo search algorithm with Lévy flights for global-support parametric surface approximation in reverse engineering, *Symmetry (MDPI)*. 10 (3) (2018) 58.
- [12] S. Fiori, R. Di Filippo, An improved chaotic optimization algorithm applied to a DC electrical motor modeling, *Entropy (MDPI)*. 19 (12) (2017) 665.
- [13] M. Beşkirli, I. Koc, H. Kodaz, Optimal placement of wind turbines using novel binary invasive weed optimization, *Tehnički vjesnik*. 26 (1) (2019) 56–63.
- [14] A.V.V. Sudhakar, C. Karri, A.J. Laxmi, Optimal bidding strategy in deregulated power market using invasive weed optimization, in: Applications of Artificial Intelligence Techniques in Engineering, SIGMA 2018. Springer Singapore, 2019;2: 421–429.
- [15] J. Midhunchakkarakaravarthy, S.S. Brunda, A novel approach for feature fatigue analysis using HMM stemming and adaptive invasive weed optimisation with hybrid firework optimisation method, *Int. J. Computer Aid. Eng. Technol.* 11 (4–5) (2019) 411–429.
- [16] H. Rezk, A. Fathy, M. Aly, M.N.F. Ibrahim, Energy management control strategy for renewable energy system based on spotted hyena optimizer, *Comput., Mater. Continua*. 67 (2) (2021) 2271–2281.
- [17] S.K. ElSayed, E.E. Elattar, Hybrid Harris hawks optimization with sequential quadratic programming for optimal coordination of directional overcurrent relays incorporating distributed generation, *Alex. Eng. J. (Elsevier)*. 60 (1) (2021) 2421–2433.
- [18] T.A. Jumani, M.W. Mustafa, Z. Hussain, M. Md. Rasid, M.S. Saeed, M.M. Memon, I. Khan, K.S. Nisar, Jaya optimization algorithm for transient response and stability enhancement of a fractional-order PID based automatic voltage regulator system, *Alex. Eng. J. (Elsevier)* 59 (4) (2020) 2429–2440.
- [19] M. Alshafeey, C. Csaba, A case study of grid-connected solar farm control using artificial intelligence genetic algorithm to accommodate peak demand, *J. Phys.: Conf. Ser.* 1304 (1) (2019) 012017.
- [20] M. D'Antonio, C. Shi, B. Wu, A. Khaligh, Design and optimization of a solar power conversion system for space applications, *IEEE Trans. Ind. Appl.* 55 (3) (2019) 2310–2319.
- [21] A.M. Eltamaly, H.M.H. Farh, M.S. Al Saud, Impact of PSO reinitialization on the accuracy of dynamic global maximum power detection of variant partially shaded PV systems, *Sustainability (MDPI)* 2019;11(7):2091.
- [22] W.A.E.M. Ahmed, M.M. Adel, M. Taha, A.A. Saleh, PSO technique applied to sensorless field-oriented control PMSM drive with discretized RL-fractional integral, *Alex Eng J (Elsevier)*. 60 (4) (2021) 4029–4040.
- [23] M.I. Mosaad, M.O. abed el-Raouf, M.A. Al-Ahmar, F.A. Banakher, Maximum power point tracking of PV system based cuckoo search algorithm: review and comparison, *Energy Procedia (Elsevier)* 162 (2019) 117–126.
- [24] M.A. Mohamed, A.M. Eltamaly, A.I. Alolah, A.Y. Hatata, A novel framework-based cuckoo search algorithm for sizing and optimization of grid-independent hybrid renewable energy systems, *International journal of green energy*. 16 (1) (2019) 86–100.
- [25] M. Mareli, B. Twala, An adaptive Cuckoo search algorithm for optimisation, *Appl. Comput. Inform.* 14 (2) (2018) 107–115.
- [26] O. Abdalla, H. Rezk, E.M. Ahmed, Wind driven optimization algorithm based global MPPT for PV system under non-uniform solar irradiance, *Solar Energy (Elsevier)* 180 (2019) 429–444.
- [27] M.H. Qais, H.M. Hasanien, S. Alghuwainem, Enhanced whale optimization algorithm for maximum power point tracking of variable-speed wind generators, *Appl. Soft Comput. (Elsevier)*. 86 (2020) 105937.
- [28] S. Mohanty, B. Subudhi, P.K. Ray, A new MPPT design using grey wolf optimization technique for photovoltaic system under partial shading conditions, *IEEE Trans. Sustain. Energy* 7 (1) (2015) 181–188.
- [29] H. Alhumade, E. H. Houssein, H. Rezk, I. A. Moujdin, S. Al-Shahrani, Modified artificial hummingbird algorithm-based single-sensor global MPPT for photovoltaic systems, *Mathematics (MDPI)* 2023;11(4):979.
- [30] A.O. Alsaiari, E.B. Moustafa, H. Alhumade, H. Abulkhair, A. Elsheikh, A coupled artificial neural network with artificial rabbits optimizer for predicting water productivity of different designs of solar stills, *Adv. Eng. Software (Elsevier)*. 175 (2023) 103315.
- [31] L. Wang, Q. Cao, Z. Zhang, S. Mirjalili, W. Zhao, Artificial rabbits optimization: a new bio-inspired meta-heuristic algorithm for solving engineering optimization problems, *Eng. Appl. Artif. Intell. (Elsevier)*. 114 (2022) 105082.
- [32] N. Boutasetta, M.S. Bouakkaz, N. Fergani, I. Attoui, A. Bouraiou, A. Neçabia, Solar energy conversion systems optimization using novel jellyfish based maximum power tracking strategy, *Procedia Comput. Sci. (Elsevier)*. 194 (2021) 80–88.
- [33] A. Fathy, H. Rezk, D. Yoursi, T. Kandil, A.G. Abo-Khalil, Real-time bald eagle search approach for tracking the maximum generated power of wind energy conversion system, *Energy (Elsevier)*. 249 (2022) 123661.
- [34] E. Turajlic, E. Buza, A. Akagic, Honey badger algorithm and chef-based optimization algorithm for multilevel thresholding image segmentation, in: 2022 30th Telecommunications Forum (TELFOR): 1–4. IEEE, 2022.
- [35] H.-Y. Wang, B. Chen, D. Pan, Z.-A. Lv, S.-Q. Huang, M. Khayatnezhad, G. Jimenez, Optimal wind energy generation considering climatic variables by Deep Belief network (DBN) model based on modified coot optimization algorithm (MCOA), *Sustain. Energy Technol. Assess. (Elsevier)*. 53 (2022) 102744.
- [36] H. Rezk, M. Aly, A. Fathy, A novel strategy based on recent equilibrium optimizer to enhance the performance of PEM fuel cell system through optimized fuzzy logic MPPT, *Energy (Elsevier)*. 234 (2021) 121267.
- [37] Y.Z. Rajam, R. Retnamony, Hybrid Approach Based Power Quality Improvement In Smart Grid Connected Renewable Energy System Using Dstatcom: A Gbdt-Poa Technique, 2022.
- [38] S. Tiachacht, S. Khatir, C.L. Thanh, R.V. Rao, S. Mirjalili, M. Abdel Wahab, Inverse problem for dynamic structural health monitoring based on slime mould algorithm, *Eng. Comput.* 38 (S3) (2022) 2205–2228.
- [39] A.M. Nassef, E.H. Houssein, B.-D. Helmy, H. Rezk, Modified honey badger algorithm based global MPPT for triple-junction solar photovoltaic system under partial shading condition and global optimization, *Energy (Elsevier)* 254 (2022) 124363.
- [40] W. Long, J. Jiao, X. Liang, M. Xu, M. Tang, S. Cai, Parameters estimation of photovoltaic models using a novel hybrid seagull optimization algorithm, *Energy (Elsevier)* 249 (2022) 123760.
- [41] T. Nagadurga, P.V.R.L. Narasimham, V.S. Vakula, R. Devarapalli, F.P.G. Márquez, Enhancing global maximum power point of solar photovoltaic strings under partial shading conditions using chimp optimization algorithm, *Energies (MDPI)* 14 (14) (2021) 4086.
- [42] A.K. Gautam, M. Tariq, K.S. Verma, J.P. Pandey, H. Malik, G. Chaudhary, S. Srivastava, An intelligent BWO algorithm-based maximum power extraction from solar-PV-powered BLDC motor-driven light electric vehicles, *J. Intell. Fuzzy Syst.* 42 (2) (2022) 767–777.

- [43] S. Murugan, M. Jaishankar, K. Premkumar, Hybrid DC–AC microgrid energy management system using an artificial gorilla Troops optimizer optimized neural network, *Energies* (MDPI). 15 (21) (2022) 8187.
- [44] Y. Houam, A. Terki, N. Bouarroudj, An efficient metaheuristic technique to control the maximum power point of a partially shaded photovoltaic system using crow search algorithm (csa), *J. Electr. Eng. Technol.* 16 (1) (2021) 381–402.
- [45] V. Gonal, G.S. Sheshadri, A hybrid bat–dragonfly algorithm for optimizing power flow control in a grid-connected wind–solar system, *Wind Eng.* 45 (2) (2021) 231–244.
- [46] K.K. Mohammed, S. Mekhilef, S. Buyamin, Improved rat swarm optimizer algorithm-based MPPT under partially shaded conditions and load variation for PV systems, *IEEE Trans. Sustain. Energy* 14 (3) (2023) 1385–1396.
- [47] Y. Zhu, M.K. Kim, H. Wen, Simulation and analysis of perturbation and observation-based self-adaptable step size maximum power point tracking strategy with low power loss for photovoltaics, *Energies* (MDPI). 12 (1) (2018) 92.
- [48] A.M. Eltamaly, A novel musical chairs algorithm applied for MPPT of PV systems, *Renew. Sustain. Energy Rev.* (Elsevier). 146 (2021) 111135.
- [49] N. Aouchiche, M.S. Aitcheikh, M. Becherif, M.A. Ebrahim, AI-based global MPPT for partial shaded grid connected PV plant via MFO approach, *Solar Energy* (Elsevier). 171 (2018) 593–603.
- [50] A.M. Eltamaly, H.M.H. Farh, M.S. Al-Saud, Grade point average assessment for metaheuristic GMPP techniques of partial shaded PV systems, *IET Renew. Power Gener.* 13 (8) (2019) 1215–1231.
- [51] N. Priyadarshi, V.K. Ramachandaramurthy, S. Padmanaban, F. Azam, An ant colony optimized MPPT for standalone hybrid PV-wind power system with single Cub converter, *Energies* (MDPI). 12 (1) (2019) 167.
- [52] B.O. Yang, L. Zhong, X. Zhang, H. Shu, T. Yu, H. Li, L. Jiang, L. Sun, Novel bio-inspired memetic salp swarm algorithm and application to MPPT for PV systems considering partial shading condition, *J. Clean. Prod.* 215 (2019) 1203–1222.
- [53] B.O. Yang, T. Yu, X. Zhang, H. Li, H. Shu, Y. Sang, L. Jiang, Dynamic leader based collective intelligence for maximum power point tracking of PV systems affected by partial shading condition, *Energ. Convers. Manage.* 179 (2019) 286–303.
- [54] M.J. Alshareef, An effective falcon optimization algorithm based MPPT under partial shaded photovoltaic systems, *IEEE Access* 10 (2022) 131345–131360.
- [55] A. Rinehart, V. Shyam, W. Zhang, Characterization of seal whisker morphology: implications for whisker-inspired flow control applications, *Bioinspir. Biomim.* 12 (6) (2017) 066005.
- [56] G. Dehnhardt, Björn Mauck, W. Hanke, H. Bleckmann, Hydrodynamic Trail-Following in Harbor Seals (*Phoca vitulina*), *Science* 293 (5527) (2001) 102–104.
- [57] H. Hans, J.M. Miao, M.S. Triantafyllou, Mechanical characteristics of harbor seal (*Phoca vitulina*) vibrissae under different circumstances and their implications on its sensing methodology, *Bioinspir. Biomim.* 9 (3) (2014) 036013.
- [58] G. Dehnhardt, B. Mauck, H. Bleckmann, Seal whiskers detect water movements, *Nature* 394 (6690) (1998) 235–236.
- [59] J.H. Solomon, M.J. Hartmann, Biomechanics: robotic whiskers used to sense features, *Nature* 443 (7111) (2006) 525.
- [60] X. Zhang, X. Shan, T. Xie, J. Miao, H. Du, R. Song, Harbor seal whisker inspired self-powered piezoelectric sensor for detecting the underwater flow angle of attack and velocity, *Measurement* (Elsevier). 172 (2021) 108866.
- [61] J. Momin, X.S. Yang, A literature survey of benchmark functions for global optimization problems, *J. Math. Model. Num. Optim.* 4 (2) (2013) 150–194.
- [62] H. Mohammed, T. Rashid, FOX: a FOX-inspired optimization algorithm, *Appl. Intell.* (Springer) 2022; 1-21.
- [63] J. Derrac, S. García, D. Molina, F. Herrera, A practical tutorial on the use of nonparametric statistical tests as a methodology for comparing evolutionary and swarm intelligence algorithms, *Swarm Evolut. Computat.* (Elsevier). 1 (1) (2011) 3–18.
- [64] M. Friedman, The use of ranks to avoid the assumption of normality implicit in the analysis of variance, *J. Am. Statist. Assoc.* (Taylor & Francis). 32 (200) (1937) 675–701.
- [65] JL. Jr. Hodges, E.L. Lehmann, Rank methods for combination of independent experiments in analysis of variance, in: *Selected works of EL Lehmann*. Springer US, Boston, MA, 2011, pp. 403–418.
- [66] H. Zaher, M.H.M. Eid, R.S.A. Gad, I.M. Abdelqawee, An alternative algorithm to invasive weed optimization based global maximum power point tracking for PV array under partial shading conditions, *Int. J. 9 (5)* (2020).
- [67] H. Zaher, M.H.M. Eid, R.S.A. Gad, I.M. Abdelqawee, Improved invasive weed optimization algorithm for global maximum power point tracking of PV array under partial shading conditions, *Int. J. Appl. Metaheuristic Comput.* (IJAMC) 13 (1) (2022) 1–21.
- [68] P.D.S. Vicente, E.M. Vicente, M.G. Simoes, E.R. Ribeiro, Shading position effects on photovoltaic panel output power, *Int. Trans. Electrical Energy Syst.* 30 (1) (2020) e12163.
- [69] O.A.M. Omar, N.M. Badra, M.A. Attia, Enhancement of on-grid pv system under irradiance and temperature variations using new optimized adaptive controller, *Int. J. Electr. Comput. Eng.* 8 (5) (2018) 2650.
- [70] M. Mandalaki, T. Tsoutsos, M. Mandalaki, T. Tsoutsos, Remarks on shading systems, *Sol. Shad. Syst.: Des. Perform. Integrat. Photovolt.* (Springer) (2020) 115–117.
- [71] F.A. Khan, N. Pal, S.H. Saeed, Review of solar photovoltaic and wind hybrid energy systems for sizing strategies optimization techniques and cost analysis methodologies, *Renew. Sustain. Energy Rev.* (Elsevier). 92 (2018) 937–947.
- [72] S. Pathy, C. Subramani, R. Sridhar, T.M.T. Thentral, S. Padmanaban, Nature-inspired MPPT algorithms for partially shaded PV systems: a comparative study, *Energies* (MDPI). 12 (8) (2019) 1451.
- [73] C.M. Rahman, T.A. Rashid, A new evolutionary algorithm: learner performance based behavior algorithm, *Egyptian Informat. J.* (Elsevier). 22 (2) (2021) 213–223.